Naval Research Laboratory

Washington, DC 20375-5000

NRL Memorandum Report 6270

WAKEX 86

A Ship Wake/Films Exploratory Experiment

J. A. C. KAISER AND W. D. GARRETT*

Space Sensing Branch
Space Systems and Technology Department

S. E. RAMBERG**, R. D. PELTZER AND M. D. ANDREWS

Center for Hydrodynamic Developments
Laboratory for Computational Physics and Fluid Dynamics

**Present Address: ORINCON, Inc., Suite 904*
1755 Jefferson Davis Hwy.
Arlington, VA 22202

***Present Address: Office of Naval Research*
Arlington, VA 22217

November 17, 1988

SECURITY CLASSIFICATION OF THIS PAGE

REPORT DOCUMENTATION PAGE

Form Approved
OMB No 0704 0188

1a REPORT SECURITY CLASSIFICATION UNCLASSIFIED	1b RESTRICTIVE MARKINGS
2a SECURITY CLASSIFICATION AUTHORITY	3 DISTRIBUTION/AVAILABILITY OF REPORT Approved for public release; distribution unlimited.
2b DECLASSIFICATION/DOWNGRADING SCHEDULE	
4 PERFORMING ORGANIZATION REPORT NUMBER(S) NRL Memorandum Report 6270	5 MONITORING ORGANIZATION REPORT NUMBER(S)
6a NAME OF PERFORMING ORGANIZATION Naval Research Laboratory 6b OFFICE SYMBOL (If applicable) Code 8312	7a NAME OF MONITORING ORGANIZATION
6c ADDRESS (City, State, and ZIP Code) Washington, DC 20375-5000	7b ADDRESS (City, State and ZIP Code)
8a NAME OF FUNDING/SPONSORING ORGANIZATION Office of Naval Research 8b OFFICE SYMBOL (If applicable)	9 PROCUREMENT INSTRUMENT IDENTIFICATION NUMBER
8c ADDRESS (City, State, and ZIP Code) 800 N. Quincy Street Arlington, VA 22217	10 SOURCE OF FUNDING NUMBERS PROGRAM ELEMENT NO 61153N 61153N PROJECT NO BR021-01-W1 TASK NO WORK UNIT ACCESSION NO
11 TITLE (Include Security Classification) WAKEX 86; A Ship Wake/Films Exploratory Experiment	
12 PERSONAL AUTHOR(S) Kaiser, J.A.C., Garrett,* W.D., Ramberg,** S.E., Peltzer, R.D., and Andrews, M.D.	
13a TYPE OF REPORT Final 13b TIME COVERED FROM 6/86 TO 12/86 14 DATE OF REPORT (Year, Month, Day) 15 PAGE COUNT 59	
16 SUPPLEMENTARY NOTATION *ORINCON, Inc., Suite 904, 1755 Jefferson Davis Hwy., Arlington VA 22202 **Office of Naval Research, Arlington, VA 22217	
17 COSATI CODES FIELD / GROUP / SUB-GROUP	18 SUBJECT TERMS (Continue on reverse if necessary and identify by block number) Ship wakes, Ocean films, Ship hydrodynamics, Remote sensing, Ship waves, Vortices, Surface tension, Hull flows

19 ABSTRACT (Continue on reverse if necessary and identify by block number)

In an exploratory experiment on Chesapeake Bay we examined several aspects of ship wakes and their interaction with natural and artificial surface films. We used aerial photography to record these interactions, the geometries of white water wakes and the motions of drifters distributed in the wakes of ships. We also measured the surface tension across ship wakes in natural waters. Our velocity measurements using the drifters are consistent with the theory (Garrett and Smith, 1984; Swanson, 1986) that a displacement hull sheds a pair of vortices which moves surface water away from the center of the wake. (Our observations of the artificial slick/wake interactions corroborate this conclusion.) On either side of the wake in natural waters, slicked bands were visually observed and measurements showed their surface tension to be several dynes/cm lower than the ambient; this indicates these slicked bands to be compacted surfactant material which damp the capillary and capillary-gravity waves. This pattern of slicked bands is very similar to those highly persistent ones photographed from space (Scully-Powers, 1986) and is consistent with the wake vortex theory. Our photographs also suggest that surfactant material is being deposited in these bands by rising bubbles which scour surfactants from the water column; these bubbles are generated by the bow wave. The white water wake observations are consistent with Peltzer 1984a but also show the importance of the bow wave in foam generation.

20 DISTRIBUTION/AVAILABILITY OF ABSTRACT ☒ UNCLASSIFIED/UNLIMITED ☐ SAME AS RPT ☐ DTIC USERS	21 ABSTRACT SECURITY CLASSIFICATION UNCLASSIFIED
22a NAME OF RESPONSIBLE INDIVIDUAL Jack A.C. Kaiser	22b TELEPHONE (Include Area Code) (202) 767-2969 22c OFFICE SYMBOL Code 8312

DD Form 1473, JUN 86 Previous editions are obsolete SECURITY CLASSIFICATION OF THIS PAGE

CONTENTS

WAKEX 86
A SHIP WAKE/FILMS EXPLORATORY EXPERIMENT

1. INTRODUCTION

Remote signatures of ship wakes obtained by various techniques most often include a long narrow feature along the ship track which is customarily associated with the turbulence. The ship track is visually rougher and more aerated in the near wake than the ambient ocean, but it then evolves to a discernably smoother region in the far wake. The linear connectedness of the overall feature makes it readily identifiable in remote sensing images. When spatial resolution permits, some sensors (SAR, RAR) exhibit crosstrack wake structure most often seen as higher intensity returns or emission from one or both edges of the feature [Hawkins *et al* (1986)], but when surface films are present, the wake edges may produce lower intensity returns.

The persistence of a discernable far wake feature in remote sensing images (several hours in photographs from the Space Shuttle [Scully-Power, 1986]) cannot be explained on the basis of a simple wave/current interaction between the mean surface wake flow and the ambient short wavelength scatterers, because the along-track mean flow diminishes too rapidly to support a simple interaction over the observed distances. Several mechanisms have been postulated to account for the observed wake persistence including special Bragg scattering effects, cross-track (transverse) mean flow structures and surface-active films. Transverse or cross-track mean surface flows are expected to stem from some combination of propeller swirl, thermal mixing and trailing vortices from control surfaces, bilges and so forth [Garrett and Smith (1984), Lugt (1981)]. These vortical motions are imbedded in the early turbulent wake but are far less attenuated than the along-track mean flow and may, therefore, emerge in the far wake as the dominant motion capable of supporting a more persistent wave/current interaction for "blocking" scatterers from the wake region.

In connection with these vortical motions it has been suggested [Garrett and Smith (1984)] that surface-active films may collect in the surface flow convergence zones which will form at the boundaries of the turbulent wake feature. Compaction of such films attenuate short wavelength scatterers and may alter the energy exchanges between capillary and gravity wave components in the ambient seas [Garrett (1967b), Huhnerfuss *et al.* (1981)]. Swanson (1986) has developed a simple model for these secondary flows which may compact films. Active radar systems will detect an absence of resonant scatterers in these films, and imaging radars that combine amplitude and Doppler signals (e.g., SAR) may discern an altered phase relationship between capillary and gravity waves.

The experiments described in this report were undertaken to examine the surface flows associated with, and the roles of, both natural and artificial films in ship wakes, and to explore small-scale ship wake experiments as a means to fill the gap between fundamental laboratory experiments and large-scale remote sensing experiments as planned for 1988. Experiments on a smaller scale also provide a low-cost means for exploring "surface truth" methods, examining basic phenomeonology, as well as an opportunity to perform selected demonstration experiments with new remote sensor systems. The future coupling of simple remote sensing demonstration experiments with "surface truth"

Manuscript approved September 13, 1988.

measurements will aid developments in both of these areas while lending some guidance to modeling efforts and planning for more complex experiments.

The WAKEX 86 experiments described in this report were performed by NRL staff members on Chesapeake Bay during three days in September 1986. In addition to the general objectives described above WAKEX 86 had a number of specific objectives, they are:

1. Obtain in-situ surface film measurements in and about the wakes of passing ships.

2. Evaluate artificial films for ship wake research.

3. Observe surface flow patterns in the wakes of both large ships and small boats to examine general features and to evaluate several techniques.

4. Evaluate aerial photographic techniques and parameters for both films and "surface truth" methods.

5. Seek sources and examine the state of natural surface-active films in and about ship wakes.

6. Obtain representative sub-surface bubble measurements.

Results for all but the last objective were obtained and are described in the following Sections of this report. The bubble measurements were not attempted for lack of an available, suitable means to obtain the data. Overall, the experiments proved very successful and cost-effective. The results suggest several processes which may be important to include in wake modeling efforts, and provide information which will aid in planning future small-scale and large-scale experiments. The various results are described in Section 3 in some detail and summarized in Section 4. Recommendations for future efforts of this nature are given in Section 5 of the report.

2. PROCEDURES AND METHODS FOR WAKEX 86

Three types of experiments were conducted during WAKEX 86: Wakes from a large (500 ft length) displacement hull were observed for their general features, surface flow patterns and organization of ambient surface films; wakes from small ships (displacement and planing hull) were studied for their general features and surface flow patterns; and lastly, displacement hull/artificial slick interactions were observed.

The experiments were conducted in Chesapeake Bay from 2 to 5 miles due east of the Naval Research Laboratory's Chesapeake Bay Detachment Facility at Randle Cliff, Maryland in the vicinity of 38°39′ North and 76°24′ to 28′ West. The experiments were run on 17 to 19 September 1986. Figure 2.1 shows these locations. Large ship wake experiments took place in the ship channel in the "wake" location shown in Fig. 2.1. This portion of Chesapeake Bay is less influenced by coastal and channel boundary effects than most portions of the Bay. Small boat wake experiments and ship/artificial slick experiments were done in the region marked "slick."

Two small boats, two aircraft, and commercial ships of opportunity were used for these experiments. The general plan was to have the two small boats (the LELAND B and the SHADY LADY) aid in the large-ship wake measurements, create their own wakes for the small-ship wake measurements, or to dispense and then drive through artificial slicks. The small boats also acted as reference markers in some cases and patrolled the area to keep other small boats away from some of the experiments.

The two aircraft were used at separate times to obtain aerial photography and to direct the small boats via two-way radio during each experiment. The aerial observer also kept a verbal log on tape. A Cessna-172 carried an observer and a photographer. The aircraft has a high wing and seats one person up front on the right of the pilot and can accommodate three people on a rear bench which spans the cabin. The observer had a lap board which contained the two-way radio, tape recorder, two 35mm cameras, a watch, pen, note pad and a sign that contained information about each roll of film. The photographer used the back bench. The observer only used the camera with a 50mm lens in the C-172 and the photographer used a Nikon with zoom lens and a data back. Verbal communication could be maintained between the pilot, observer and photographer. Both the observer and the photographer were knowledgable about the phenomena to be photographed. All 35mm photos were taken through the closed cabin windows because the noise from an open window made communication in the cabin or via two-way radio impossible.

The second aircraft used was a Cessna-180 outfitted with a 9 in format mapping camera and a 152mm lens. The C-180 was also a high-wing aircraft but could only carry one person in addition to the pilot. In that case the same person functioned as observer and photographer at some expense in communication among participants. The pilot actuated the mapping camera and aligned the aircraft using a small viewing port in the floor of the aircraft.

During ship wake measurements the C-180 (with mapping camera) was flown, but during artificial film/ship wake interaction studies, the C-172 was used for better slant photography and observation. The C-180 flew on 17 and 19 Sept. and the C-172 on 18 Sept.

Three different types of experiments were performed as indicated in Table 2.1: Large ship wake (LSW) experiments, small ship wake (SSW) experiments and ship/artificial slick (SAS) interaction experiments.

Table 2.1 — Experiment Schedule

Local time	Date		
	17th	18th	19th
1000	SWW		SWW
1100	SSW		
1200		SAS	
1300	LSW		LSW
1400	SAS		
1500	SSW		

During these experiments we took slant photography (SP) with the 35mm cameras through the aircraft windows, vertical photography with the Fairchild mapping camera (MP), dispensed markers (M), made surface tension (ST) measurements and characterized the environment (E) in a simple way. During the three types of experiments these observations and techniques were employed as listed below in Table 2.2.

Table 2.2 — Measurement Plan

	Experiment		
	LSW	SSW	SAS
Measurements:	SP	SP	SP
	MP	MP	E
	M	M	
	ST	E	
	E		
Aircraft:	C-180	C-180	C-172

These measurements are described in the following Sections along with methods of data reduction and interpretation.

2.1. Slant Photography

Two hand-held 35mm cameras were used to obtain photographs through the side windows of either the Cessna 172 or 180. One camera, a Pentax K-1000, had a standard 50mm lens with no filters. Exposures were determined with the through-the-lens metering system. The exposure was occasionally reset if lighting conditions appeared to change. Kodak Ektachrome, ASA 64, daylight film was used to produce 35mm transparencies.

The second camera was a Nikon Model F-3 equipped with a battery-powered motorized film advance and a data back which printed day, hour, and minute on the film. An 80-200mm zoom lens was used with an ultraviolet filter. Exposures were determined automatically with the through-the-lens metering system. Generally a fast shutter (1/500 or 1/1000 sec) and a slower aperture was used to eliminate aircraft vibration and motion influences on the photographs. Kodacolor VR-G 35mm print film was used. From the negatives sharp prints up to 8 in × 10 in can be obtained.

2.2. Mapping Photography

To photograph the markers (also called drifters in this report) and foam in the wakes of large ships or small boats, a Cessna-180 equipped with a Fairchild T-12 mapping camera was used. The camera had a 6-in (152mm) focal-length lens and was mounted in a frame which could be leveled in flight. The camera was triggered remotely by the pilot. Frames could be taken about 2 s apart. Each frame also contained a record of the altitude, time of day, exposure number, and date. The aerial image on the film is 9 in × 9 in which gives very high resolution for an image spanning 1.5 times the altitude. Most photographs with the mapping camera were taken from 650 to 1000 ft altitude, so that the frames cover a surface area of about 1000 to 1500 ft on a side. Fig. 2.2 is a sample of a photo taken with the mapping camera. This camera format was chosen to evaluate very high spatial resolution photographs for purposes of establishing "surface truth" and to provide plan-view images with little or no geometric distortion. Unexpected distortion on the order of 5 to 10 percent became apparent in the images during data reduction and have introduced some uncertainties in those results as discussed in the next Section.

In a typical wake photographic sequence, the C-180 would fly up the wake and as the markers came into the field of a viewing port in the aircraft floor, 3 or 4 photos would be taken at 2 to 5 s intervals. Then another pass was made putting the C-180 over the marker field several minutes later. Up to five passes were made for one wake condition.

2.3. Surface Flow Markers

The markers or drifters that were used to tag the surface flow in and around the ship wake were 1 ft squares of 1/4 in thick plywood. They were indented on one side near a corner to provide a handle so that they could be readily distributed by throwing into the ship wakes. The markers were painted with a flat light yellow latex paint and numbered from 1 to 100 in black paint. As Fig. 2.2 shows, the numbers were not visible from our standard mapping photograph altitudes but did prove useful in the retrieval of the markers after each deployment; this retrieval was mandated by environmental considerations. The markers could be distributed up to 70 ft or so by an average person when thrown overhand in a vertical orientation, and this is how they were distributed in the large ship wakes.

Each of the small boats converged on the stern of the passing ship from opposite sides as shown in Fig. 2.3. The boats coasted into their final deployment positions outside the apparent turbulent wake region (indicated by the visible white-water and foam lines as shown in the aerial photograph of Fig. 2.2) and distributed the drifters. In the small boat tests, the markers were distributed from the stern of the wake-generating boat. About 50 drifters were used for the large wakes and about 25 for the small wakes.

Several methods were used to provide reference markers in the vicinity of the deployed drifters both for use by the aircraft during the overflights and by the image data reduction. For the small boat tests, the second boat acted as a reference, while for the large ships, each small boat deployed a large white foam buoy attached to a weight which was lowered to the bottom while distributing the drifters.

The drifter coordinates were obtained from enlarged photographic prints using a digitizing tablet and pen. The reference markers were digitized along with the locations of each drifter set when available. Two checks for consistency in the data revealed an apparent image distortion and apparent movement of one or both of the reference markers during the large ship experiments. The first check of the data was to examine correlations of the distance between "fixed" reference markers and the indicated aircraft altitude. The product of this distance and altitude should be invariant with position on the film or in time if there is no distortion. Trends with elapsed time and with position in the image were identified as shown in Fig. 2.4 for example. Averages over subsets of the drifter data were expected to eventually converge to equivalent results representing the tidal drift during the experiment. This was not the case and different groups of drifters exhibited significantly different apparent tidal drift. Since the groups were identified with different positions in the photographic negative, this tended to confirm the image distortion problem although the possibility of ambient shear around the shipping channel cannot be ruled out.

An estimate of the image distortion was obtained by assuming that all distances could be scaled by the aircraft altitude and that the drifter field changed negligibly in the 2 or 3 s between successive frames. In this way the "same" drifter pattern moved across the photograph, and the distortion could be measured and approximately corrected. The average displacements (in X and Y) versus time of three groups of drifters from the 19 September experiment are plotted as points in Fig. 2.5, after this correction has been applied. The tidal drift is represented by the straight lines. Deviations from these straight lines are seen early and late. The early deviations are due to the ship wake velocities wherein the drifters are moving toward the receding ship on average (approximately opposite to the tide) and toward the edges of the wake. The deviations very late are attributed to the wide disperal of the drifters and to the uncertainties in the aircraft heading during those flights, and the image correction procedure. The ship track was no longer readily visible to the aircraft at these late times, and the passes occurred at various headings and put the markers in various positions in the photograph unlike

the earlier sequences where the markers generally moved through the center of the image along the same path. The simple image correction was based on the early frames and isn't likely to be valid across wider, different image segments. Ambiguities and uncertainties of this nature can easily be avoided in future experiments with independent image calibrations and with better reference deployments as discussed in Section 5.

2.4. Surface Films

The surface tension value is a measure of the concentration of film-forming chemicals on the surface of the water. These surfactant chemicals are produced *in situ* by various life forms in the water column. The surfactants are naturally adsorbed to and removed from the water surface by several ambient mixing processes including diffusion. The surface concentration is a result of these competing processes with the addition of any film material brought to the surface by rising bubbles; adsorption also occurs very effectively within the water column to the surface of rising bubbles. Clean water has a relatively large surface tension, about 72 mN/m [1 dyne/cm = 1 milli Newton/meter). As natural surfactants accumulate and are compacted on the surface, their presence can reduce the surface tension of the water by as much as 20 mN/m.

Of the several techniques developed to measure surface tension, the simplest for *in situ* use involves deploying a minute amount of one of a series of oils which spread or don't spread on the water surface depending upon the ambient surface tension. If an oil spreads, the ambient surface tension is greater than the value associated with the oil and another higher surface tension oil is tried. Eventually a sufficiently high surface tension oil will be found which does not spread; then the surface tension is less than the value for this non-spreading oil but greater than the value for the preceding spreading oil. Figure 2.6 shows a spreading oil above and a non-spreading oil below. The simplest way to use the oils is to dip a toothpick into one of them, toss it on the water surface and observe whether the oil spreads off of the toothpick (as in Fig. 2.6a) or does not (Fig. 2.6b). This was done from the bow of the LELAND B as it drifted ahead at 1 to 2 kn.

For our measurements Dr. William Barger of NRL's Chemistry Division prepared a set of oils having the following spreading surface tensions: 74.0, 73.0, 72.4, 71.0, 70.3, 69.0, 68.1, 66.1, 64.0, and 62.4 mN/m. A value of surface tension determined with this set of oils is nominally bracketed within a 1 mN/m bin.

2.5. Environmental Parameters

During the experiments the environment was characterized very simply. The air temperature and wet bulb temperature were measured with an aspirated psychrometer, the wind speed with a hand-held anemometer, and the surface water temperature and the water column temperature with Sippican type T-11 fine structure expendable bathythermograph probes.

3. DISCUSSION OF RESULTS

During the three day period three types of experiments were conducted: Large ship wake measurements, small boat wake measurements, and the interactions of a small boat wake with an artificial slick. These experiments and the results for each are described separately in the following sections.

3.1. Large Ship Wake Experiments

The wakes of two large (>500 ft long) ships were examined, one on the 17th and one on the 19th of September. Information on the ships (name, departure times from the pilot stations, speed,

estimated time of arrival in our operational area) was obtained from the Maryland Pilots Association in Baltimore, MD. We then confirmed the presence of the target in the area and its approximate speed using the land-based radar at the Chesapeake Bay Detachment. Following marker deployment (Section 2.3) the LELAND B proceeded upwake about 500 ft and drifted across the wake at 1 to 2 kn to start surface tension measurements using the spreading oils (Section 2.4). Fig. 3.1 shows the LELAND B starting across the wake of the first large ship. The edges of the large wake are outlined by the two reflective bands running from the center to the bottom of the photo. The SHADY LADY proceeded about 1000 ft ahead and then cut across the wake from the opposite side and commenced to sample the subsurface (2 m depth) water in the wake as it slowly drifted across the wake. This procedure is illustrated in Fig. 3.2. The 500 ft separations between the drifters, the surface tension measuring location, and the water sampling location ensured that any of these operations would not interfere with the measurements at the other location. The LELAND B went back and forth across the wake several times until the edges of the wake could no longer be detected from the surface boat or from the air. Then the LELAND B and SHADY LADY went back to the marker field and retrieved all the markers. Overflights of the marker field occurred up to the point of retrieval.

On 17 September the VENUS DIAMOND, a 650 ft long vehicle carrier with a 95 ft beam and a 28 ft draft, was observed while bound north with cargo at about 14 kn. On 19 September the wake of the CHARTER OAK, a 750 ft long tanker, heading north at 12.5 kn was measured. The CHARTER OAK's beam was 105 ft and its draft was 29 ft. It appeared to be empty or lightly loaded (ballasted).

According to Lloyds Register of Shipping, both ships evidently have single screws with deadweight displacements of 12,304 and 60,880 tonnes, respectively. We have taken the effective ship displacements for the two wakes to be about 12,000 tonnes for the VENUS DIAMOND and about 50,000 tonnes for the CHARTER OAK. These values were used to make simple comparisons to available models and to compare wake features.

For both wakes the weather was quite settled. Figure 2.3 shows the passage of the VENUS DIAMOND on the 17th. The surface of the Bay shows many natural slicks; the wind was about 3 kn from the northwest and the waves were less than 30 cm. The air temperature was 18°C and the water temperature 14.5°C. On the 19th the wind was 6 kn from the west, the waves were 30 cm or less, the air temperature was 19.5°C, and the water at the surface was 21.0°C.

3.1.1. Marker measurements — The second large ship marker deployment (Sept. 19th, CHARTER OAK) was better executed and included both reference marker placements. Only those results are presented and discussed here. Following digitization and correction as described in Section 2.3, five realizations of the distributed marker field positions were differenced to obtain four sets of displacement fields as shown on the left side of Fig. 3.3 through 3.6. A reference length of 64 m for the displacements is shown in Fig. 3.3. The corresponding average Lagrangian velocities in the axial (along-track) and transverse (crosstrack) directions for each marker were obtained by dividing their displacement by the interval between overflights (typically 3-5 min). The velocity results are also plotted on those figures, and the time listed in each case is the average time of the two realizations (overflights) measured from the ship passage. One minute "time-late" corresponds to about 0.39 km or 1.7 ship lengths.

The observed velocities contain components due to the tide which were calculated from the mean long-time drift of the entire marker field (see Section 2.3). The values of the tide components along-track and cross track are indicated on the figures by the vertical dashed lines. The observed marker velocities were non-dimensionalized by these values in the appropriate directions. The ship wake velocity profiles are hand-faired curves using the tide component as the datum and with the

imposition of some symmetry about the wake axis. The data exhibit asymmetry which may be a residue of the image distortion, reference marker movement or ambient shear. Even with these uncertainties and the long averaging intervals, the plotted profiles are qualitative indications of the actual surface flow field. However, the methods can be easily improved to reduce uncertainties in future measurements (see Section 5.1).

The two horizontal axes in the figures are drawn through the locations of the two reference markers which were tethered to bottom-resting weights and positioned just outside the visible wake during marker deployment. Within the wake the markers always have an axial component toward the receding ship and opposite to that component of the tide. Initially, the wake velocities exceed the tide so the markers moved upwake absolutely, but later as the wake velocities decreased, they moved down wake absolutely.

The observed axial velocity data is always consistent with a drag-type surface velocity stemming from the deficit created by passage of the hullform. The thrust region(s) of the wake originating from the propeller(s) are submerged initially and appear to remain so throughout the observation interval. Since the turbulent wake of a surface ship is over-thrusted to balance losses due to wave-making resistance, one expects the far wake to eventually reflect a flow away from the ship. This is not seen in the data up to 10 min (4km) after ship passage. Recent simulations of the turbulent wake of a twin screw destroyer hull-form by Swean (1987) has shown that the surface "broaching" of the thrust wake component depends greatly on the direction of rotation of the two propellers. For the case where the thrust region broachs early enough to give significant velocities, the surface flow pattern shows a thrust region along the wake centerline with narrow drag-type regions on either side. If a similar structure occurred for the single-screw CHARTER OAK, it would not be readily seen in the data due to the lateral marker movements and long averaging times which could combine to yield an *underestimate* of the larger axial velocities, either drag or thrust. Moreover, the lateral spreading depleted the center of the wake of markers at later times and determinations of velocities there (drag or thrust) become sparse. Attempts to identify trends in individual marker movements which would be consistent with a combination of drag and thrust axial velocities at the surface were frustrated by these uncertainties in the data.

Estimates of the maximum axial (U_m) and lateral (V_m) velocities at times late scales with respect to the initial maxima (U_0 and V_0) were obtained from the data and are plotted in Fig. 3.7. The maximum axial velocity decays as approximately t^{-2} (or x^{-2}) which is considerably greater than what is expected for a purely drag wake. This supports the notion of a complex velocity profile where an outwardly migrating group of markers encounters axial velocities of both drag and thrust directions.

The observed lateral wake velocities do not exhibit such reversals, but, since the magnitudes are much smaller and of opposite sign on opposite sides of the wake, they are very sensitive to image rotation due to unknown shifts of one or both reference markers. This source of error grows as the markers move further away from the references and at 10 min (Fig. 3.6), clearly, such an error in V_m appears; so this data point is not plotted in Fig. 3.7.

Within the limitations of the data, it is still possible to make meaningful comparisons with a recent attempt by Swanson (1986) to model a pair of trailing vortices generated in the wake through a lift force due to set-down or "squat" of a ship underway. According to Swanson's model, the lateral wake velocities of a ship similar to the CHARTER OAK would be of the same magnitude or larger than the axial velocities at the distance corresponding to 10 min behind the ship. The data obtained here clearly does not support that result. On the other hand the observed rate of decay of the lateral velocity ($x^{-5/4}$) is greater than would be expected for a simple swirling turbulent flow ($x^{-3/4}$) but it is comparable to the "fast" decay rated for a trailing vortex pair as presented by Swanson. Thus, the

present results are consistent with a weak, rapidly decaying vortex structure that could be responsible for organizing surfactants into bands alongside the turbulent wake edges. Sustenance of the banded slick structure by vortex and/or propeller-induced flows will be weak due to the rapid decay of V_m.

3.1.2. Film pressure measurement — Figure 3.8 is a sequence of photos taken of the wake of the CHARTER OAK. As the ship passes, two rows of foam are generated at the bow (Fig. 3.8a). This foam persisted as two patchy bands for about 8 min (Fig. 3.8b and c). After the foam had largely dissipated, the edge of the wake could still be visually discerned as a narrow slick (Fig. 3.8d) for more than 20 min after ship passage, but then those slicks or edge bands became ruffled and discontinuous.

The LELAND B made seven crossings of the CHARTER OAK wake to measure ambient surface tension by the method described in Section 2.4. These measurements were from 6 to 22 min after the ship passage. Each crossing of the wake took about 2 min. During each crossing about 10 determinations of spreading oil behavior were made. The data for each crossing was examined individually, and the three earliest crossings as a set were compared to the three latest crossings. No readily detectable difference was observed, so our crossings are assumed all to be in the "late" wake as far as surface films are concerned.

The measured change of surface tension, γ, across the wake of the CHARTER OAK is shown in Fig. 3.9. Surface tension is plotted vertically and distance across the wake horizontally. The bands are the slicked regions near the wake edges shown in Fig. 3.8b-d; they were several meters wide. Each time a toothpick is thrown on the surface, the calibrated oil spreads (S) or does not (N). Each realization is plotted in Fig. 3.9 as an S or N at the point corresponding to the surface tension value for that particular oil and approximate position in the wake. The actual surface tension lies on the line which separates the N's from the S's. In the central portion of the wake of the CHARTER OAK, the data of Fig. 3.9 shows $\gamma > 72.5$ mN/m; hence the water is cleaned or unfilmed (this is shown as a dashed line). In the slicked bands $\gamma < 68$ dyne/cm, on the right side but on the left side γ varies from about 67 to less than 70 dyne/cm (the shaded portion). Earlier measurements of undisturbed water showed γ varied from 69 to 71 dyne/cm. The change of γ at the 'inside' edges of the bands are very sharp. It is not clear if this is the case on the outer edges of the bands, although Figs. 3.1, 3.8c and 3.10 would imply both edges of the bands are equally sharp.

Figure 3.10 is a photo of the LELAND B and her wake. Here the foam and the edge bands are quite discernable. These bands only become visible in a very small range of viewing angles (10° to 20°). This is a good example of the value of a highly maneuverable aerial viewing platform to observe many aspects of a complex phenomenon such as a ship wake.

The surface tension measurements in the wake of the other large ship, the VENUS DIAMOND, revealed the same pattern. In the two bands, which were each 2 to 3 m wide, $\gamma < 64$ mN/m and the ambient surface tension away from the wake was 68 to 69 mN/m. The center of the wake was clean water ($\gamma > 72.4$ mN/m.) During these measurements the winds were 3 kn compared to 6 kn for the CHARTER OAK. During the low wind-speed measurement periods, the ambient surface film pressure, π ($\pi = \gamma_{clean} - \gamma_{ambient}$) was 3 to 4 mN/m, while during the higher wind speeds $1 \lesssim \pi \lesssim 3$ mN/m, so one could collapse both sets of wake surface tension data onto a curve such as shown in Fig. 3.11. The environmental film pressure is (γ_{clean}). For our measurements $\alpha = .02$ to .04 at 3 kn and .04 to .06 at 6 kt (see Fig. 3.11 for a definition of α). The quantity r is a measure of the intensity of the compaction of the surface film by the ship wake. For both our wakes $r \approx 2$.

The slicked bands at the edge of the wake are regions of reduced surface tension and hence regions where the ambient surface films have been compacted. Presumably this compaction is due to

a secondary lateral flow, such as the surface flow from a pair of vortices generated by the hull. As a film is compacted (area decreased), its film pressure, π, increases. One π, A-curve for a natural film is shown in Fig. 3.12 (from Garrett, 1967b). Given such a curve for the material on the water surface, then from $\gamma_{ambient}$ we can calculate π and estimate A, a measure of the compactness of the film. As the film becomes compacted, the capillary damping curve of Fig. 3.12 shows an increased damping rate, and this increased damping of the capillaries produces the visible slick.

Another example which clearly shows the suppression of capillaries in the edge bands is the glint photograph shown in Fig. 3.13. The points of glitter are specular reflection of the sun from the facets of the steeper capillary waves. Figure 3.13 shows the water surface cut by the wake of the LELAND B from upper left to lower right. The wake edges appear as two parallel bands of reduced glitter (at arrows) and the residual foam from the LELAND B's wake can be seen in the center of these slicked bands.

3.1.3. Foam/Bubble observations — Figure 3.14 is a survey camera photograph of the CHARTER OAK taken from an altitude of about 2000 ft. The large format camera in a vertical look without a sun-glitter pattern can be used to determine overall features of the foam/white-water wake and to discern many of the details. More details can be revealed through enlargement and it is possible to obtain area coverages by foam late into the wake for comparison to emissivity sensor systems (e.g. - passive microwave radiometers). A view of this type does not provide the depth of the foam layer or the bubble sizes, but the depths may be estimated from gray-level variations if individual foam/white water patches can be resolved in an enlargement. Emissivity variations are largely determined by the characteristics of the uppermost bubble layer so that area coverages together with estimates or surface observations of bubble sizes will yield an adequate basis for comparison to other emissivity sensors.

The wake shown in Fig. 3.14 is typical of the two large ship experiments and of other ships and boats observed on the Bay wherein two, very persistent foam lines are created that spread very slowly downstream. The origins of the foam lines appear to be in the flow about the bow and perhaps the hull rather than the stern or propulsion. The white water/foam generated at or near the stern dissipates more rapidly and may eventually be carried to the wake edges by the transverse surface flow field. Further discussion and comparisons of the large and small ship foam wakes are given in Section 3.2.2.

Figure 3.15 shows photographs of two similar barges in transit on the same day and area of the Bay. In one case the barge is being towed and in the other the barge is being pushed which provides a qualitative comparison of differences due to propulsion on the same type of hullform. The upper photograph indicates that at least as much foam/white water is generated by the hull as by the propulsion and this tends to be swept into or near the foam lines generated at the bow. Other interesting features in these photographs include the single foam line in the lower photograph from the earlier passage of another ship and the asymmetric interaction of the tugboat wake with the bow of the barge in the lower photograph.

3.1.4. Wake samples — As mentioned in the introduction, an attempt was made to obtain subsurface water samples in and out of the visible wake region. We were seeking variations in surfactant concentrations that might indicate a "scrubbing" of surfactants from the water column by the rising wake bubble population. This mechanism is very effective and could bring higher concentrations of surface active materials to the surface and then to the edges of the wake as opposed to a simple collection of surface materials by surface flow convergence. The procedure was to bottle and mark samples extracted from a stream being pumped steadily from a depth of about 2 m. A drop of chloroform was added to halt biologic activity and the sample was sealed. Upon return to the dock the samples were allowed to stand for an hour or so, and surface tension measurements were then taken. Consistent trends could not be seen although this could well be a result of the crude method used.

One method to determine small differences in the concentration of surfactants in bulk water between samples is to measure the pressure, area isotherms of each sample. Each sample will produce a curve similiar to the solid curve of Fig. 3.12. The sample with the smaller concentration will have its pressure, area isotherm displaced in the direction of smaller film area (to the left). In using this technique, special care must be exercised. The samples must be treated identically; specifically, before they are poured into the trough used for determining the pressure, area curves, they must be thoroughly mixed. After they are poured into the trough, all samples should sit the same amount of time before being measured.

Such a set of measurements could fairly easily be included in any wake measurement program. This information coupled with subsurface bubble populations would be valuable in assessing the importance of bubbles in influencing surface signatures in ship wakes.

3.2. Small Ship Wake Experiments

The two small boats, the LELAND B and the SHADY LADY, were also used to obtain surface flow patterns and photographs of the visible wake (e.g., foam). There were advantages in having complete control over the target and measuring boats. The small ship wake experiments allowed us to develop proficiency in, and explore procedural improvements of, the various tasks that went into the large ship experiments as well as collecting useful data. The specific goal of these experiments was to again seek secondary surface flow patterns and, in particular, to compare the results for the small boats to the large ship results and to each other. A comparison between the small boat wakes was of special interest because the SHADY LADY would rise to a plane at her highest speeds in contrast to the LELAND B which remained a displacement hull throughout her speed range. The significance of the planing condition is that the direction of rotation of any trailing vortices (secondary flows) are, in principle, opposite to that of a displacing hull and would, therefore, manifest very different drifter patterns (Swanson, 1986). Such differences were not seen.

3.2.1. Marker measurements — A variety of speeds for both boats were used; they were not precisely measured, but estimated by the operators. The speeds were nominally 3, 7, and 10 kt for each boat with an additional higher speed for the SHADY LADY estimated to be about 13 or 14 kn when the boat rose to a plane. During these experiments about 25 markers were distributed over the wake from the stern of the target (wake generating) boat as it passed the stationary boat. One or two markers were thrown outside the wake to provide further references. In several runs two sets of markers were deployed.

The apparent image distortion in the mapping camera (see Section 2.3) and the lack of fixed reference markers precluded the accuracy which would be necessary to resolve the extremely small, if any, secondary motions which may have occurred. At no speed for either boat did the markers organize themselves into a pattern of any sort although foam lines and bands of surface-active materials were clearly present.

A typical result is shown in Fig. 3.16 for a 10 kn run with the LELAND B. The first three photographs taken for this sequence contained the boat and the first image occurred during the marker deployment. During the digitization of these images the outline of the boat was also plotted. For simplicity not all of the markers are plotted and in some cases markers are missing because they were not distinguishable from the foam and white water (color coding in future experiments would be useful in this regard as discussed in Section 5). The marker field in this run was photographed again on two later overflights and, within the image distortion, it was basically unchanged during the later overflights; so only the first pass of the later overflight is plotted here as the fourth data set. Distances were scaled by the altitude and no image correction was applied so the absolute distance

between the third and fourth data sets is not well-known. In this run the markers tended to be organized into three distinct laterally spaced groups as indicated on the figure. Within one to four boat lengths, there is an absence of significant surface lateral velocities as is apparent. The final data set plotted (at 156s) does suggest that the middle group experienced a slightly larger axial flow in the direction of the boat heading as one might expect, but this is clearly a very small differential surface velocity. The magnitude of the apparently simple uniform diffusion of the pattern with time is uncertain owing to the concomitant displacement of the two markers above the rest and presumably outside the wake. These were dispensed outside the wake to serve as reference markers. If the scale of the data was reduced arbitrarily to bring the upper markers more into line and thereby "correct" the image, the apparent diffusion would be nearly halved. This illustrates the large uncertainty in the image data. This sequence is typical of all the drifter data from the small boat experiments and does not give, early or late, any evidence of significant secondary flows in contrast to the large-ship wake marker results discussed earlier.

3.2.2 Foam/Bubble observations — Mapping camera photographs of the LELAND B (lower) and the SHADY LADY (upper) are shown in Fig. 3.17 for their respective top speeds, about 10 and 14 kn. At this speed the SHADY LADY is a planing hull. In each case the white water and foam appear to stem from three major sources; the bow wave, the stern wave and the stern propulsor(s). Of the three, the bow and stern waves are the strongest and most persistent contributors to the visible far wake and define a visible wake width, W, which is readily obtained from the photographs. Scaling W by the ship's beam, B, values of W/B versus distance, x/L are plotted in Fig. 3.18 for the small boat runs described above and the earlier two large chip cases (see Section 3.1.3). When nondimensionalized in this way, three separate curves are obtained. The two large ships exhibit about the same visible wake growth to about three beam widths, whereas the LELAND B wake grows to about seven beams and the SHADY LADY to over nine beams. In all cases the visible wake included the surfactant bands which appeared to be vestiges of the earlier white water/foam streaks arising from the bow and stern waves (bow waves only for the large ships). This wake existed throughout the sequence of images used to obtain the data shown in Fig. 3.18 and thus the limits indicated on the figure are the ends of the photo sequence and the actual wake lengths were longer. With the proper viewing angle (c.f. Fig. 3.10) the surfactant bands are seen to exist for much longer. The limits of data in Fig. 3.18 more closely represent the limit of visibility for a vertical look although this also depends on the sun's incidence angle.

The actual dimensions of all four visible wakes were about the same so that the different curves in Fig. 3.18 are largely a result of differences in the ship beams and lengths. If each set of wake width data is normalized by some early width, then all four curves become similar and suggests that the dominant generating processes are the bow (and possibly stern) waves to establish the visible wake and that a variety of bubble/foam/film processes determine its persistence. This renders the visible wake independent from the usual ship parameters. It must be noted that a correlation based on ship draft and/or power expended in the bow and stern waves may be required for a full accounting of the generation processes.

3.3. Artificial Film Experiments

Two artificial films were dispensed on the Bay during these tests by pumping slick-forming material directly into the wake of the LELAND B as she made way across the wind at 10 kn. The slicks were about one statute mile long. Figure 3.19 shows the LELAND B laying out the second slick.

Two liters of oleyl achohol (9-octadecen-1-ol,cis isomer) were used to generate each of the experimental slicks. By calculation it was determined that the slicks contained a six-fold excess of

film-forming material over that required for a monomolecular layer at a film age of 8 min and a two-fold excess at 40 min film age. Even though an excess of material is applied to the water surface, the effective slick is one molecule in thickness.

The film-forming liquid, oleyl alcohol, was selected on the basis of a number of physical and chemical criteria, one of which required that the material be autopholic; i.e., the excess liquid does not spread over its own monofilm, but remains on the water surface as a bulk drop in spreading equilibrium with the film. Thus, the floating excess droplets represent a reservoir of material to rapidly replace losses of the spread film when caused by disruptive environmental processes such as wind and waves. The second slick, 11 min old, is shown in Fig. 3.20 as the higher reflectivity (lighter) band extending upward from left to right. The wind speed was 6 to 8 m/s during the second slick experiment. Note that the wind has started to make inroads on the windward (upper) side. Presumably the streaks which appear to be breaking up the slick in a spatialy regular pattern are surface manifestations of Langmuir cells. During these slick/wake interaction experiments, three phenomena were observed: (1) The parting of the slick in the wake, (2) the suppression of wake foam by the slick, and (3) an unusual wave pattern which may or may not be related to the slick.

3.3.1. Parting of the slick — For each slick, the LELAND B was driven through the slick at 10 kn after allowing 11 to 14 min for the slicks to spread naturally. Fig. 3.21 is a sequence showing four LELAND B cuts through the artificial slick on the 17th. The four cuts were done between 1421 and 1426 local time (the day of the month & the local hour & minute are printed in the lower right corner by the camera data back.) The first cut, the left-most of Fig. 3.21a and the one in Fig. 3.21b, clearly show that the boat opens a path through the slick material and this material does not close back in over the cut in the first 5 min. At 9 min the first cut is still clearly visible in Fig. 3.21c. Other later cuts also can be seen in the slick at 1429.

Figure 3.21b shows the "classical" pattern of organization of a surface film by a displacement hull. Two bands of the film material are organized on either side of the wake, and the center of the wake is clear of any film. Another similar series for the same slick is shown in Fig. 3.22. Figure 3.22a and b show the LELAND B cutting through the slick. At 1454 and 1458 the cut can still be seen. These patterns would show up more clearly if viewed from a lower grazing angle. This is seen in Fig. 3.22d where another boat is cutting a swath through natural slicks in the background (from right to left at the arrow). The view of the extended wake is reminiscent of the Scully-Power photos from STS-41G. A similar wake-slick interaction pattern was observed on the 18th. The LELAND B initially cut though the slick at 1154 and its swath is still clearly seen at 1207 as the diagonal cut through the left end of the slick in Fig. 3.23.

Two possible mechanisms may be involved in the parting of the surface slick material; the lateral currents generated at the ship's bow and the lateral flow produced by a pair of vortices shed behind the displacement hull. The bow flow certainly will part the film, but evidence such as Figs. 3.8a and 3.10 suggest that the slick bands observed on either side of the wake may be organized by the bow wave rather than being formed by the flow associated with a pair of shed vortices in the wake. The marker observations in the wake suggest there is a lateral flow in the wake which could be a result of a pair of vortices and could sustain the slick bands over long periods of time by holding the bands in compaction against the water outside of the wake. The subsurface bubbles generated in the bow wave and stern wave may also scavenge surfactants from the water and deposit them at the surface.

These observations suggest the following mechanism of wake band formation and maintenance: The bow wave removes some surface material from the hull area and concentrates it in the bands on either side of the white water wake. Further behind the ship, surface flow from the vortices remove

more surface material from the center of the wake and concentrates it in the edge bands. The bubbles created by the bow and stern waves may also scavenge surfactants from the water, and as they rise to the surface and remain visible as foam, these scavenged surfactants are largely deposited in the wake and edge bands. The vortices will eventually advect any surfactants in the wake out to the edge bands. For relatively calm seas the residual vortex flow will compact the surfactants film material against the water outside the wake, and a weak stress counter to that of the vortices is necessary to disperse the edge bands since they are held together by a very weak force of cohesion. In modeling ship wakes all these mechanisms must be included.

3.3.2. Suppression of wake foam — As the LELAND B crossed both artificial slicks at 10 kn, the bands of foam on either side of the wake were completely suppressed. Figure 3.24 shows two views of the crossing of the first slick; the slick was 15 min old and had an equivalent thickness of about 5-7 molecules. Figure 3.24a is a few seconds earlier than 3.24b; note that the foam and bubbles are completely suppressed.

Figure 3.25 is a sequence showing the LELAND B crossing the second slick. This slick was 14 min old and also had an equivalent thickness of 5 to 7 molecules. The suppression of foam and bubbles is again evident in the slick which appears slightly darker in the first three photographs and lighter in the fourth.

Measurements of the lifetime of bubbles rising through various surface films were performed in the laboratory (Garrett, 1967c). Films were spread on water surface and their film pressures varied with a movable barrier. Single bubbles of different sizes were allowed to rise to the surface from a 1 cm depth in a hydrophil tray and their residence times (τ) at the surface (time of impact on the surface to time of bursting) measured. The time τ varied as the film pressure changed as shown in Fig. 3.26, which is for oleic acid. As the film became compressed (film pressure increased), the bubble lifetimes decreased rapidly, and at large film pressures (30 dyne/cm) when the film becomes compacted, bubble lifetimes are just several seconds; this is consistent with our observations of oleyl alcohol slicks.

Garrett (1967c) also measured the lifetimes of bubbles with natural slick-forming materials and found longer times, especially in organically-rich natural water. These measured lifetimes are still short compared to the observed lifetime of foam in the ship wakes outside of artificial slicks, typically several minutes. But another difference existed between the natural and artificial slick case during our experiments. The artificial slick case corresponds precisely to the laboratory measurements of Garrett (1967c) in that the surface film existed before the bubbles rose to it, whereas the natural films were collected together by the wake secondary flow concurrently with the bubbles rising to the surface and forming foam.

Another difference between the two cases is the nature of the film. Oleyl alcohol is insoluble in water, whereas most natural film materials are soluble to some extent. This difference can be very important in foam formation since the soluble compounds can drastically increase foam persistence (e.g., detergents). These observations suggest an interesting application of film technology for the Navy to manage observability of white water wakes through dispersal of film forming chemicals during certain critical times. Since one molecule of oleyl alcohol covers about 22 square angstroms and one liter contains 3.16 moles of the material, one liter will cover about 8 km of a 50 m wide wake. Further investigations of the interactions of natural and artificial films with a broad spectrum of bubble sizes are needed to fully interpret these observations.

3.3.3. "Fan Waves" — When the LELAND B drove through the second artificial slick at 10 kn an interesting pattern was observed and recorded in the slant photographs. This pattern is especially

pronounced in Figs. 3.25c and 3.25d to the right of the boat as viewed from ahead. This pattern appears to be a manifestation of the Kelvin wake brought out by the viewing angle, the slick, the earlier acceleration or turn, or some combination of these factors. The feature is noted here for the record and should be sought again as part of any future experiments of this kind where the same or similar circumstances can be re-created.

4. SUMMARY

We conceived and performed WAKEX 86 to gain experience with small-scale ship wake experiments, to develop methods of "surface truth" measurement, and to explore wake hydrodynamics with emphasis on secondary lateral flows, especially those which might explain Scully-Power's, sun-glint photographs. These studies included drifter measurements. Simple procedural improvements have been determined for each of these techniques which would be very useful in future ship wake experiments at any scale.

All of the observations with large ships and small boats show the most persistent wake feature to be a pair of bands of surfactant material aligned with the ship track along the edges of the so-called turbulent far-wake. The bands are each typically one to several meters wide and appear to be vestiges of the white water and foam streaks that eminate from the breaking bow and/or stern waves.

Surface drifter measurements of the ship wakes indicate a transverse or secondary flow pattern which would aid in the organization and sustenance of compacted surfactant bands. Similar surfactant bands were observed for the smaller boat wakes without accompanying secondary flows. The mean transverse or secondary flows were not resolved as well as possible. There is evidence that the weak transverse flows are more persistent than the axial flows which supports the notion of some trailing vortex structure in large ship wakes.

The far wake geometry of these bands is apparently determined mostly by the near wake white water geometry to the extent that the smaller boats could generate nearly the same far wake band separations as the much wider and longer ships. This implies a dependence upon selected ship characteristics (e.g. - bow and stern waves, draft, etc.) for the generation of these features and a primary dependence on bubble, foam, film, and oceanographic parameters for the persistence of these features.

Experiments with artificial films and small boats revealed similar far wake behavior with the exception that bubbles and foam formation were suppressed. This is predictable on the basis of laboratory experiments by Garrett (1967c) who used a very similiar insoluble surfactant material (oleic acid). The persistence of foam and bubbles in natural ship wakes is not fully understood but may depend strongly on the constituents of natural surfactants which may include soluble and thus more foam stabilizing chemicals. In any case artificial slicks may be exploitable as a means to suppress selected wake features under certain conditions.

5. RECOMMENDATIONS

5.1. General

The experience and results gained by WAKEX 86 provide a basis for improving some of the methods employed as well as a basis for recommending future experiments of this nature. Recommendations for improvements in the techniques and procedures are discussed below, but first, our experience has provided suggestions for future small-scale wake experiments. An essential ingredient to any future experiments is the concomitant use of remote sensing systems(s) to provide at least

preliminary correlations with the surface observations. Since these systems are likely to be flown for testing purposes prior to any large-scale wake experiments, numerous opportunities would be available for cooperative efforts given the relative simplicity of arranging the small-scale wake experiments. One highly desirable improvement, but which could make these tests less readily arranged, is the use of a cooperating "large" ship to obtain full control over its schedule and the operating parameters. These small scale experiments, such as the one we performed in September 1986, serve as a natural link between tank experiments, where basic physics in its simplest form is explored, and the real world which is very complex. These small-scale experiments are also inexpensive—ours cost $25K (excluding salaries).

Although the Chesapeake Bay location offers a number of convenience advantages, another site has been considered near the mouth of the Bay about 15 miles offshore where there is a Coast Guard tower in about 20 m of water. This tower has been used by NRL researchers in the past but is presently unmanned. It could serve as a fixed reference and a stable platform in more "open" ocean conditions.

5.2. Procedural Improvements

The following paragraphs list and briefly describe improvements in techniques and methods that would be useful in future small-scale or large-scale wake experiments.

5.2.1. Improved marker techniques — Three modifications are necessary for improving marker measurements in future experiments. They are: camera calibrations, better reference marking and more frequent realizations, especially in the early wake. Camera calibrations can be readily obtained by overflights of a known land target pattern (e.g. - marked parking lot). Use of fixed buoys and reference markers deployed prior to ship passage would be very useful. In deep water this is not practical so we suggest deployment of long buoyant cables along the outsides of the wake during marker distribution. This type of distribution would best be performed from the target ship itself and would result in markers bracketed by references of known total arc length and frame-to-frame orientation. A second and later release of markers in the center of the water to replace those convected to the edges would be desirable. The need for more frequent images cannot be met with a camera aboard a single small aircraft. To avoid difficulties of using multiple aircraft it seems more plausible to use some other aerial platform such as a helicoptor or perhaps even a tethered balloon arrangement.

Other improvements might include color coding of the markers and concomitant video recording of the marker field. This would serve to better locate markers in the midst of white water and to help reconstruct motions of individual markers. A qualitative measure of the vertical gradient of velocity very near the surface might be obtained by additional markers whose drag elements are effectively some distance below the surface. In any case some simple tests with the markers to indicate their response to combined winds, waves, and currents would be useful.

5.2.2 Improved surface tension measurements — The existing technique is very slow. A small amount of spreading oil is put on the water surface by dipping a toothpick into the oil and throwing it on the water surface. It either spreads or it doesn't. Then other oils are repeatedly tried until the surface tension is bracketed between the values corresponding to those two contiguous oils which do and don't spread. A special array should be built and tested which will place about 15 different oils on the surface at one time. Then the surface tension will be bracketed each time the array is applied to the water surface. The results will be recorded on a video recorder; this allows a more careful evaluation of the spreading oil patterns and archival of the raw data.

Also, during the wake experiments film samples should be collected and a rough (~5 point) film pressure, area-curve determined using a specially designed trough on board the ship. From this curve the surface elasticity modulus can be estimated which is important in order to evaluate the effects of the film on the wave fields in and out of the wake.

6. ACKNOWLEDGEMENTS

The experiments and analyses reported here were supported by the Naval Research Laboratory, Codes 121 and 122 of the Office of Naval Research, and the Defense Sciences Office of the Defense Advanced Research Project Agency.

7. REFERENCES

Adamson, A.W., 1976, *Physical Chemistry of Surfaces*, third edition, John Wiley and Sons.

Akers, R.J., editor, 1976, *Foams*, Proceedings of a Symposium, Sept. 8-10, 1975, Academic Press.

Alpers, W.R., Ross, D.B. and Rufenach, C.L., 1981, On the detectability of ocean surface waves by real and synthetic aperture radar, J. Geophys. Res., *86*, 6481-6498.

Barger, W.R., Daniel, W.H. and Garrett, W.D., 1974, Surface chemical properties of banded sea slicks, *Deep Sea Research*, *21*, 83-89.

Bickerman, J.J., 1973, *Foams*, Springer Verlag New York.

Cooper, A.L., 1986, Interactions between ocean surface waves and currents, NRL Memorandum Report 5755.

Garrett, W.D., 1967a, The organic chemical composition of the ocean surface, *Deep Sea Res.*, *14*, 221-227.

Garrett, W.D., 1967b, Damping of capillary waves at the air sea interface by oceanic surface-active material, *J. Mar Res.*, *25*, 279-291.

Garrett, W.D. 1967c, Stabilization of bubbles at the air-sea interface by surface-active material", *Deep-Sea Res.*, *14*, 661-672.

Garrett, W.D. and Barger, W.R., 1970, Factors affecting the use of monomolecular surface films to control oil pollution on water, *Environ. Sci. Techn.*, *4*, 123-127.

Garrett, W.D. and Smith, P.M., 1984. Physical and chemical factors affecting the thermal IR imagry of ship wakes, NRL Memorandum Report 5376.

Hawkins, S., A.F. Petty and C.S. Weller "Sea-Surface Signature Experiment SIR-B/K 1049 (U)" NRL Report 9003, Sept. 30, 1986 (Confidential).

Huhnerfuss, H., Alpers, W., Jones, W.L., Lange, P.A. and Richter, K., 1981, The damping of ocean surface waves by a monomolecular film measured by wave staffs and microwave radar, *J. Geophys. Res.*, *86*, 429-438.

Lyden, J.D., Lyzenga, D.R., Shuchman, R.A. and Kasischke, E.S., 1985, Analysis of narrow ship wakes in Georgia Strait SAR data, ERIM Topic Report No. 155900-20-T, Ann Arbor, MI.

Lugt, H.J., 1981, Numerical modeling of vortex flows in ship hydrodynamics - A review, Third International Conference on Numerical Ship Hydrodynamics, Paris.

National Defense Research Committee Division 6, 1969, *Physics of Sound in the Sea*, Part IV-Acoustic Properties of Wakes, Summary of Technical Report Vol. 8, 1946, reprinted as NAV-MAT Report P-9675.

Newman, J.N., 1970, Recent research on ship wakes, Eighth Symposium on Naval Hydrodynamics: Hydrodynamics in the Ocean Environment, Office of Naval Research, Dept. of the Navy.

Pandey, P.C. and Kakar, R.K., 1982, An empirical microwave emissivity model for a foam-covered sea, *IEEE J .Oceanic Engr.*, *OE-7*, No. 3, pp. 135-140.

Peltzer, R.D., 1984a, White water wake characteristics of surface vessels, NRL Memorandum Report 5335.

Peltzer, R.D., 1984b, Remote Sensing of the USNS *Hayes* Wake, NRL Memorandum Report 5430.

Scott, J.C., 1975, The role of salt in whitecap persistence, *Deep Sea Res*, *22*, 653.

Scully-Power, P., 1986, Navy oceanographer shuttle observations STS 41-G: Mission Report, NUSC Technical Document 7611.

Swanson, C., 1986, The effect of persistent ship wake currents on SAR imagry, Applied Physics Technology Report 6, McLean, VA.

Swean, T.F., 1987, Numerical simulations of the wake downstream of a twin-screw destroyer model, NRL Memorandum Report 6131.

Valenzuela, G.R., Plant, W.J., Schuler, D.L., Chen, D.T. and Keller, W.C., 1985, Microwave probing of shallow water bottom topography in the Nantucket Shoals, *J. Geophys. Res.*, *90*, 4931-4942.

Vesecky, J.F. and Stewart, R.H., 1982, "The observation of ocean surface phenomena using imagery from the SEASAT synthetic aperture radar: An assessment", *J. Geophys. Res.*, *87*, 3397-3430.

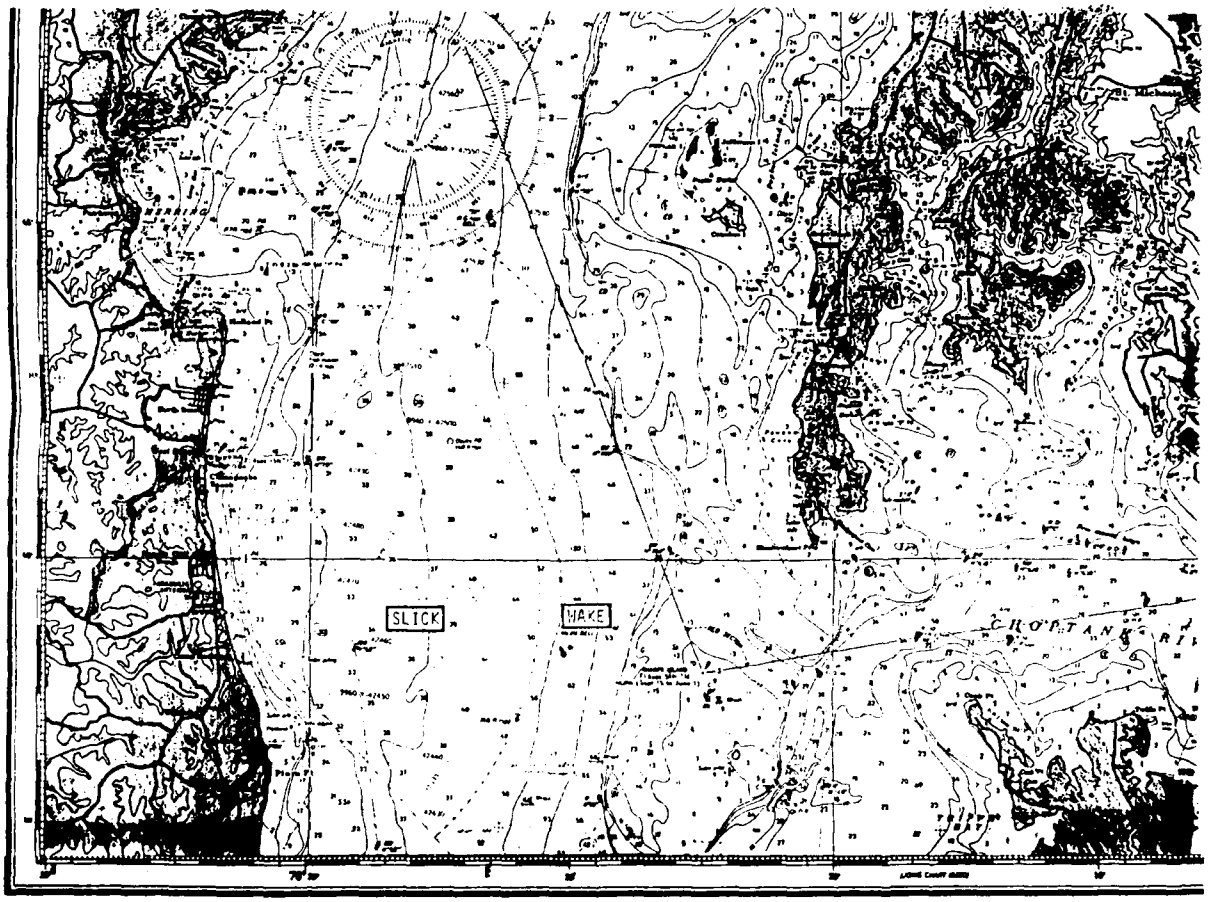

Fig. 2.1 — Locations of the WAKEX 86 artificial slick and wake experiments on Chesapeake Bay

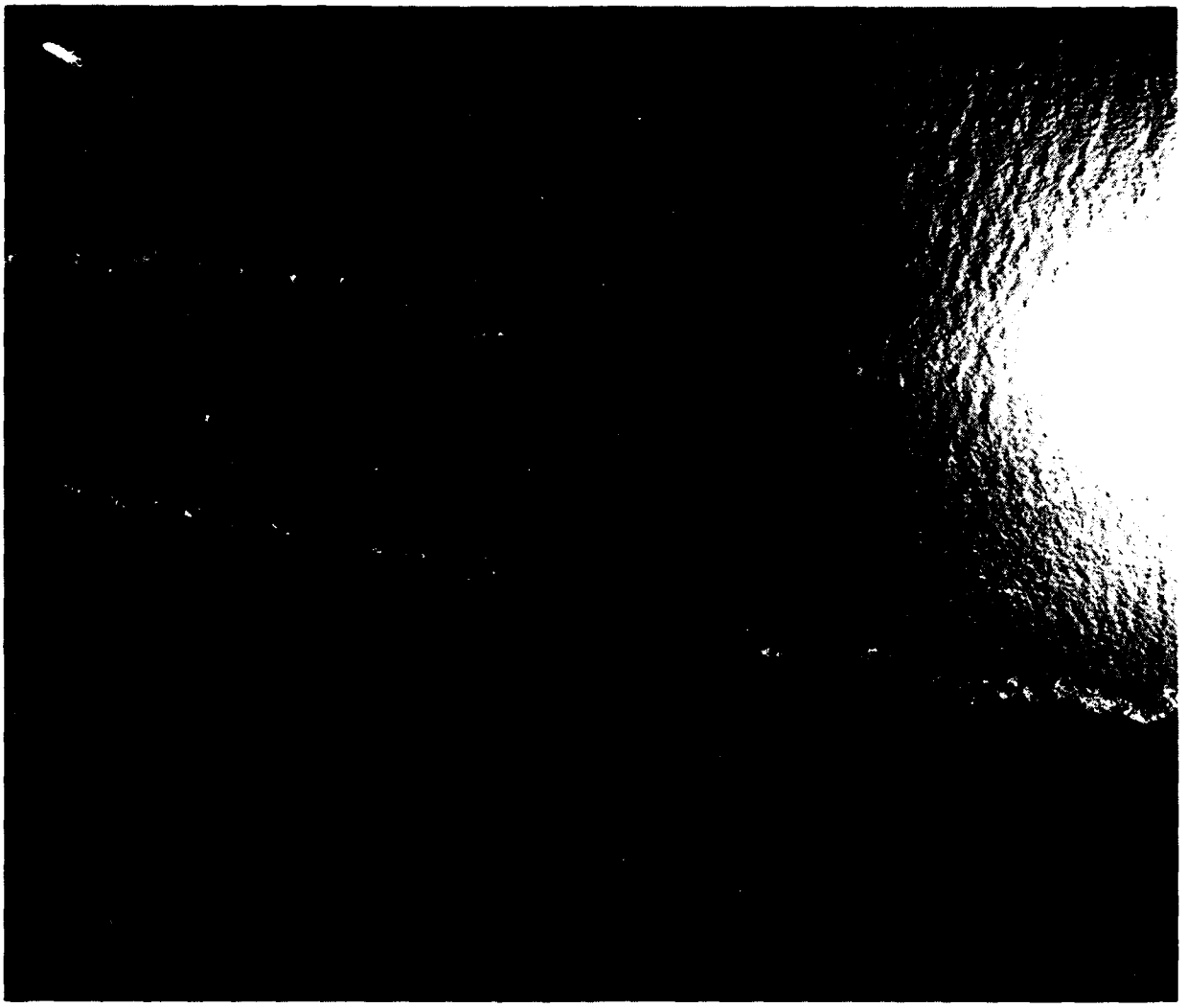

Fig. 2.2 — A sample frame from the 9″ mapping camera taken from 1050 ft and reproduced 72% of full size. The foam bands are from a large ship wake, the SHADY LADY is in the upper left, and the sun-glint pattern appears on the right. The cluster of white dots across the center of the wake is drifters.

Fig. 2.3 — Our two small boats closing on the wake of the VENUS DIAMOND to distribute markers in the large wake before commencing surface tension measurements and water sampling

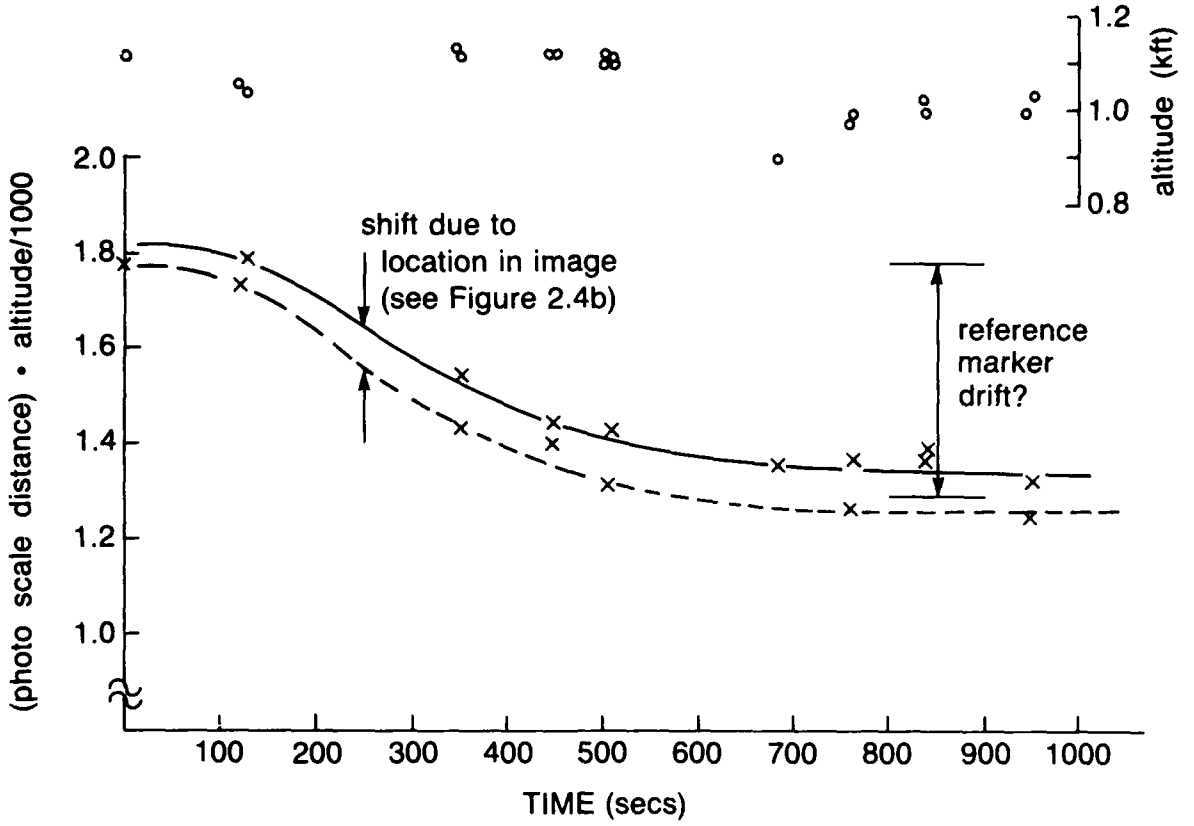

Fig. 2.4a — Apparent distance (photo scale distance x altitude) between "fixed" reference markers versus time showing unexpected trends and variations

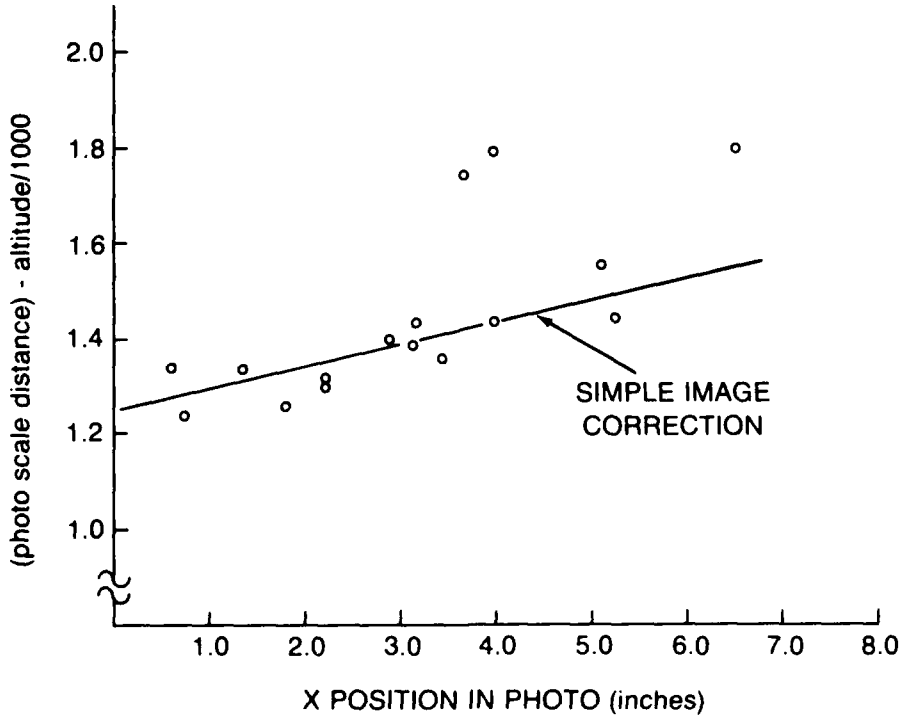

Fig. 2.4b — Apparent distance between "fixed" reference markers as a function of position on the negative. The straight line is an empirical correction for the camera distortion.

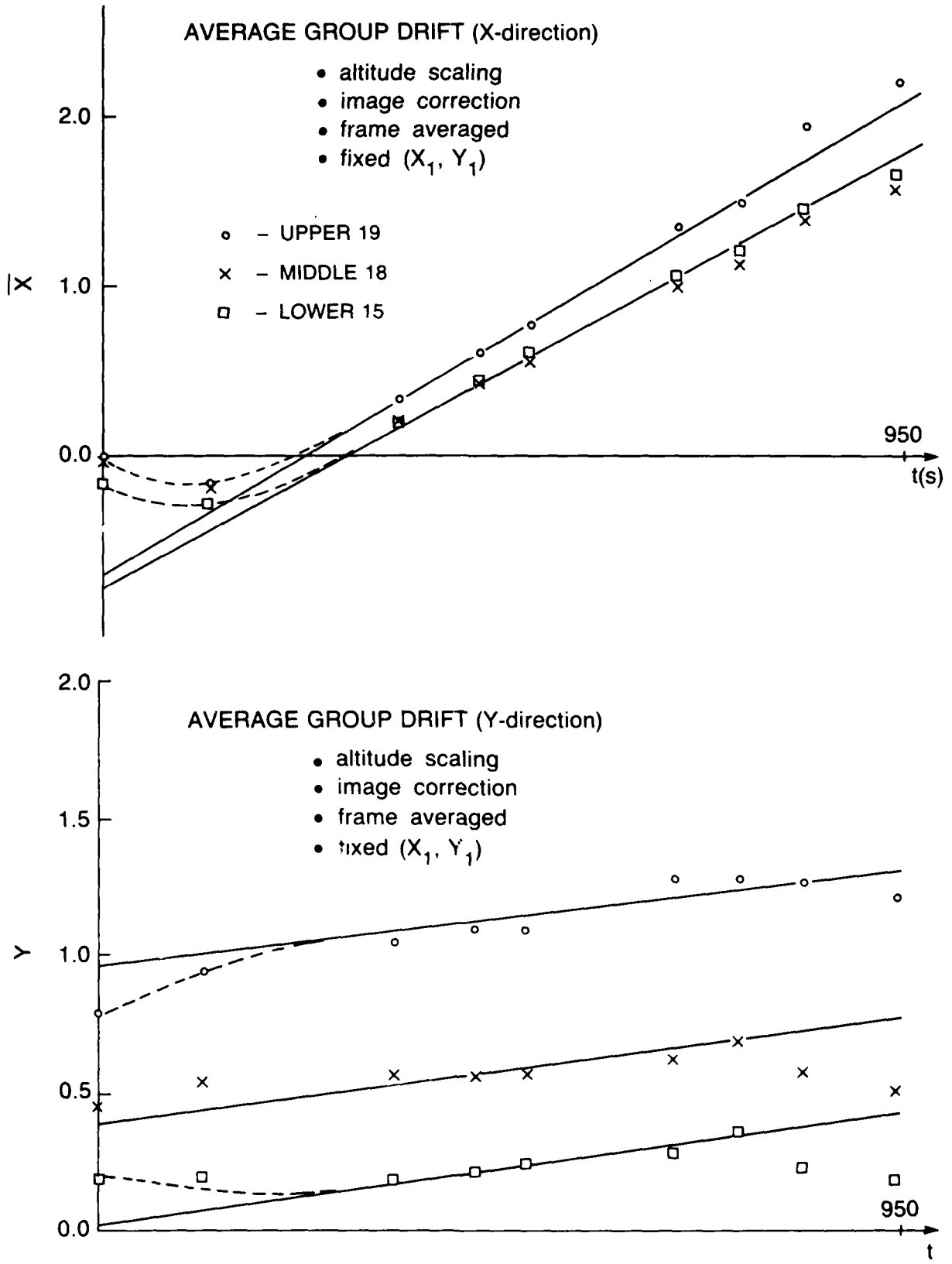

Fig. 2.5 — Corrected average marker displacements in x and y for three groups of markers (upper, middle and lower) *behind the ship* CHARTER OAK *showing tidal components*

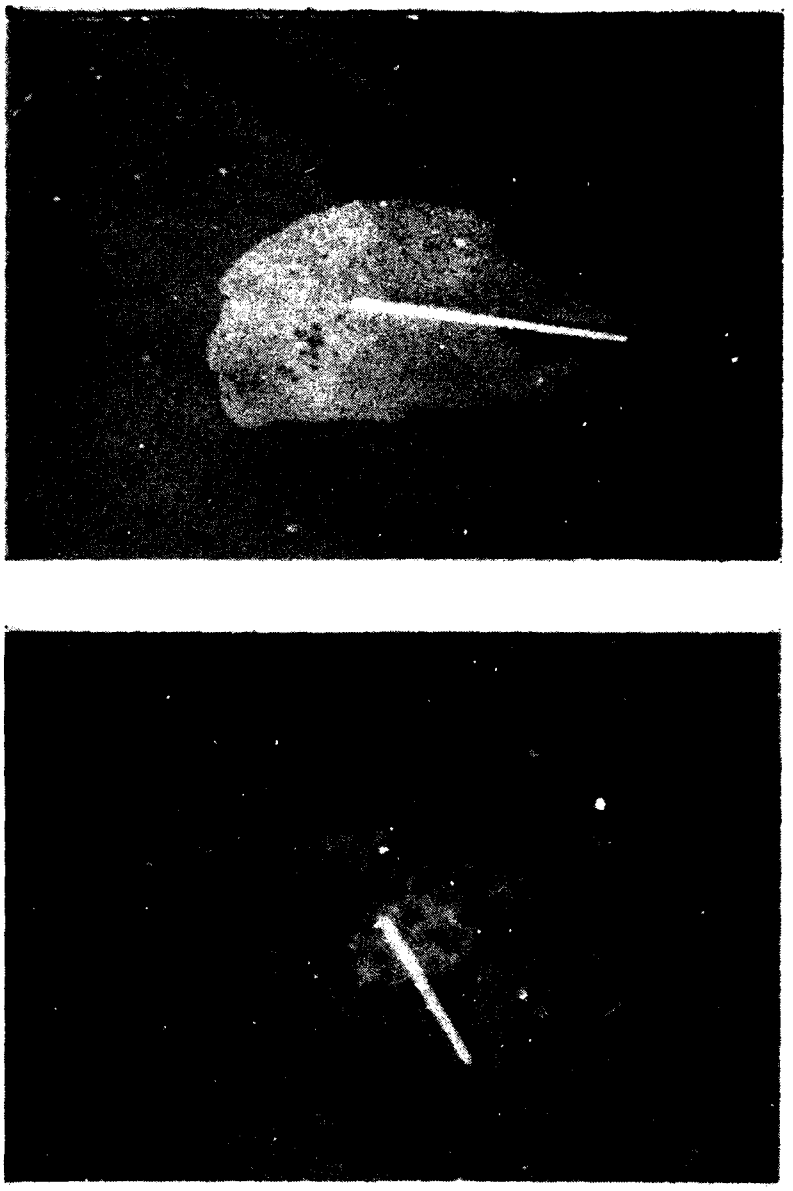

Fig. 2.6 — Photographs of calibrated spreading oils on the water surface used to bracket surface tension. The toothpick used to apply the oil to the surface is visible. In *a*, the oil spreads, so the water surface tension is greater than that indicated by the oil, while in *b*, the oil does not spread so the water surface tension is less than the oil value.

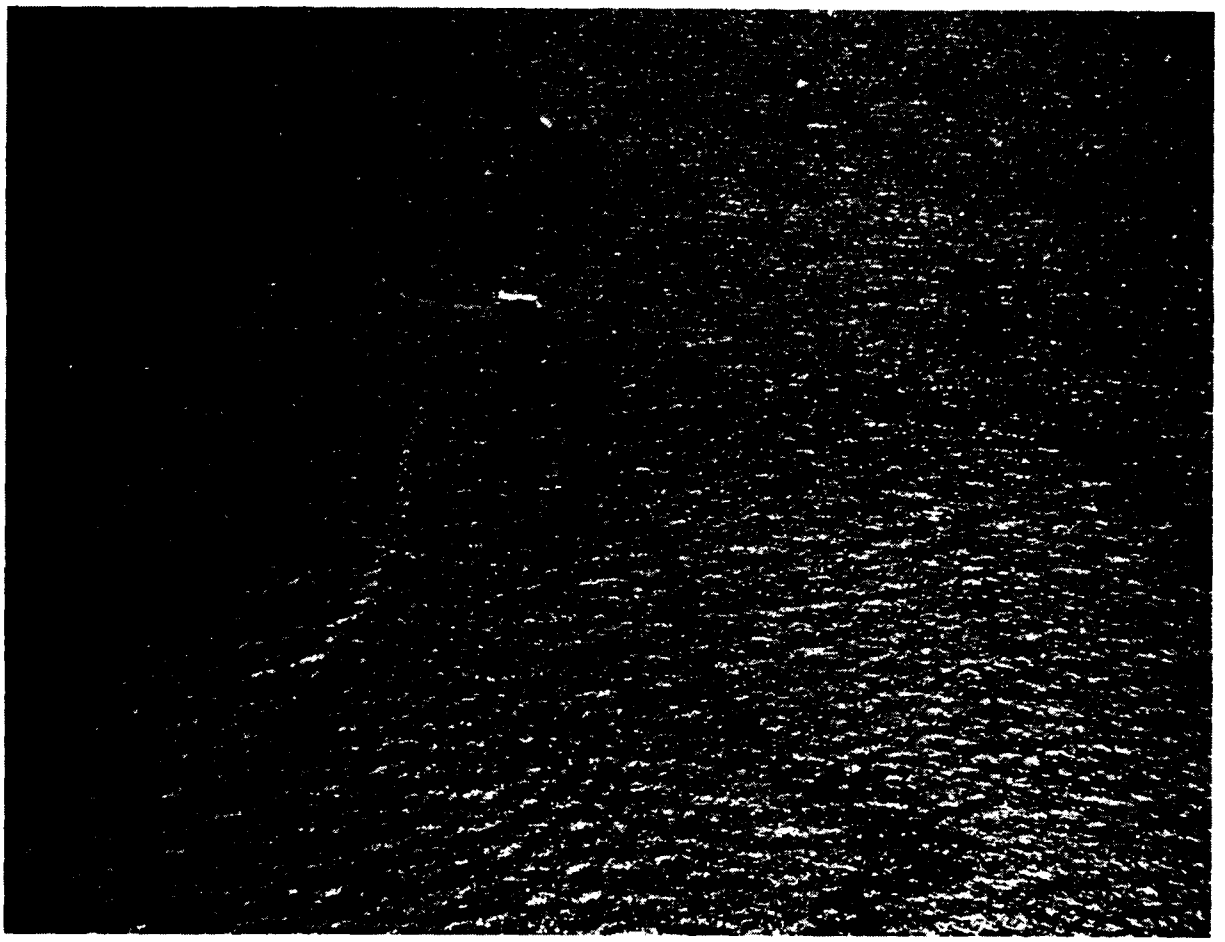

Fig. 3.1 — LELAND B turning to cross the wake of the VENUS DIAMOND to run a surface tension section of the wake. Both edge bands of the large ship wake are clearly visible.

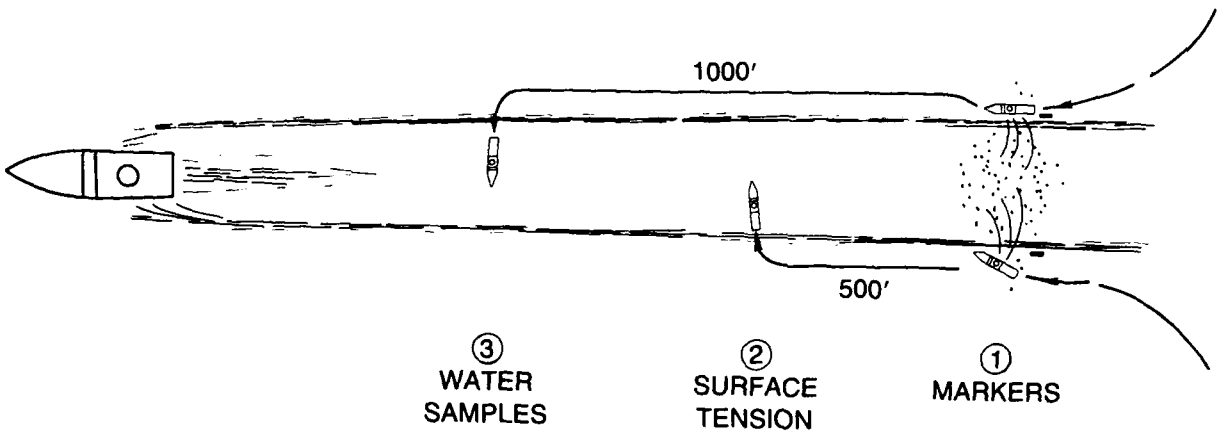

Fig. 3.2 — A schematic representation of our large ship measuring procedure using the two small boats

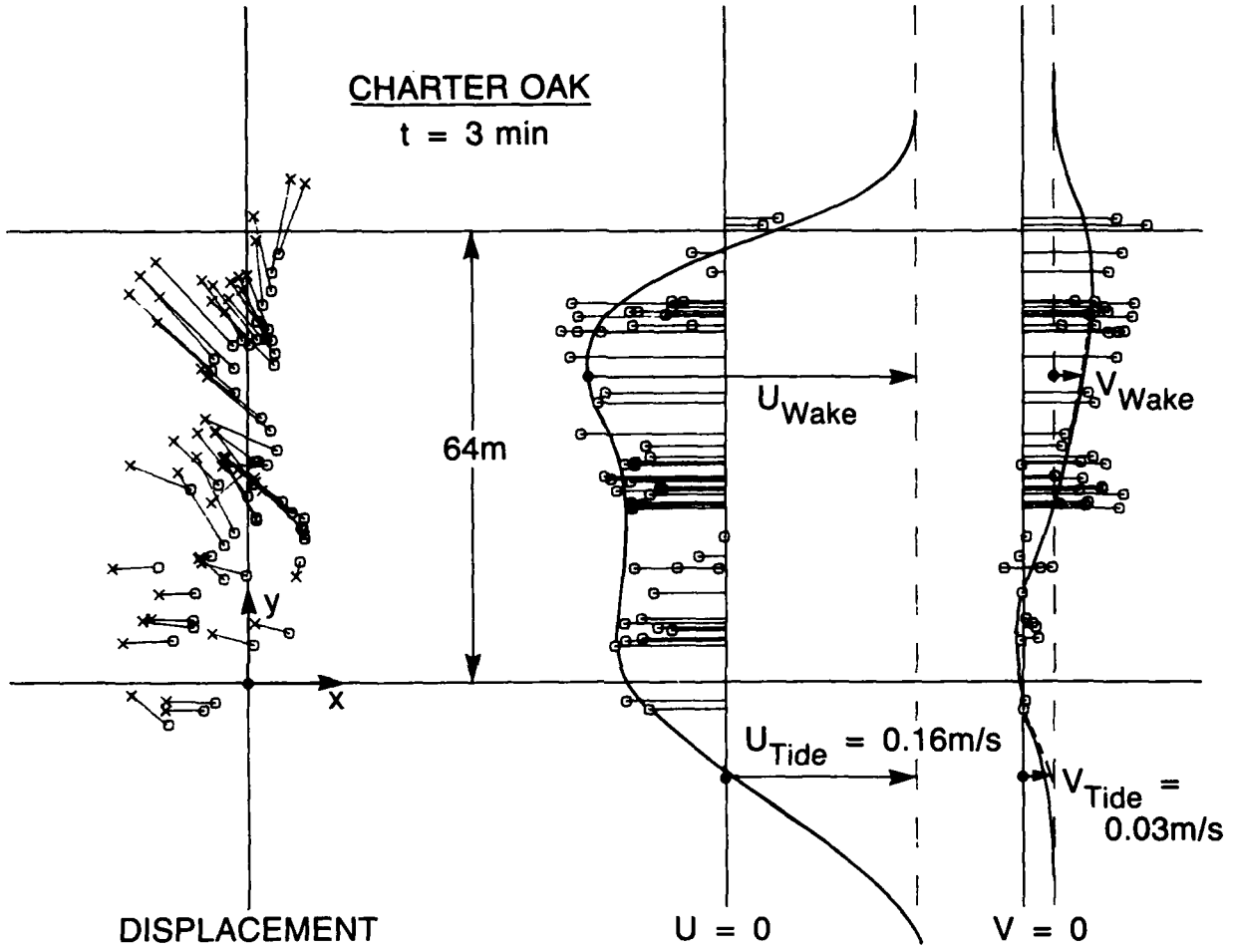

Fig. 3.3 — Marker displacements and velocity components in wake of CHARTER OAK 3 min after ship passage

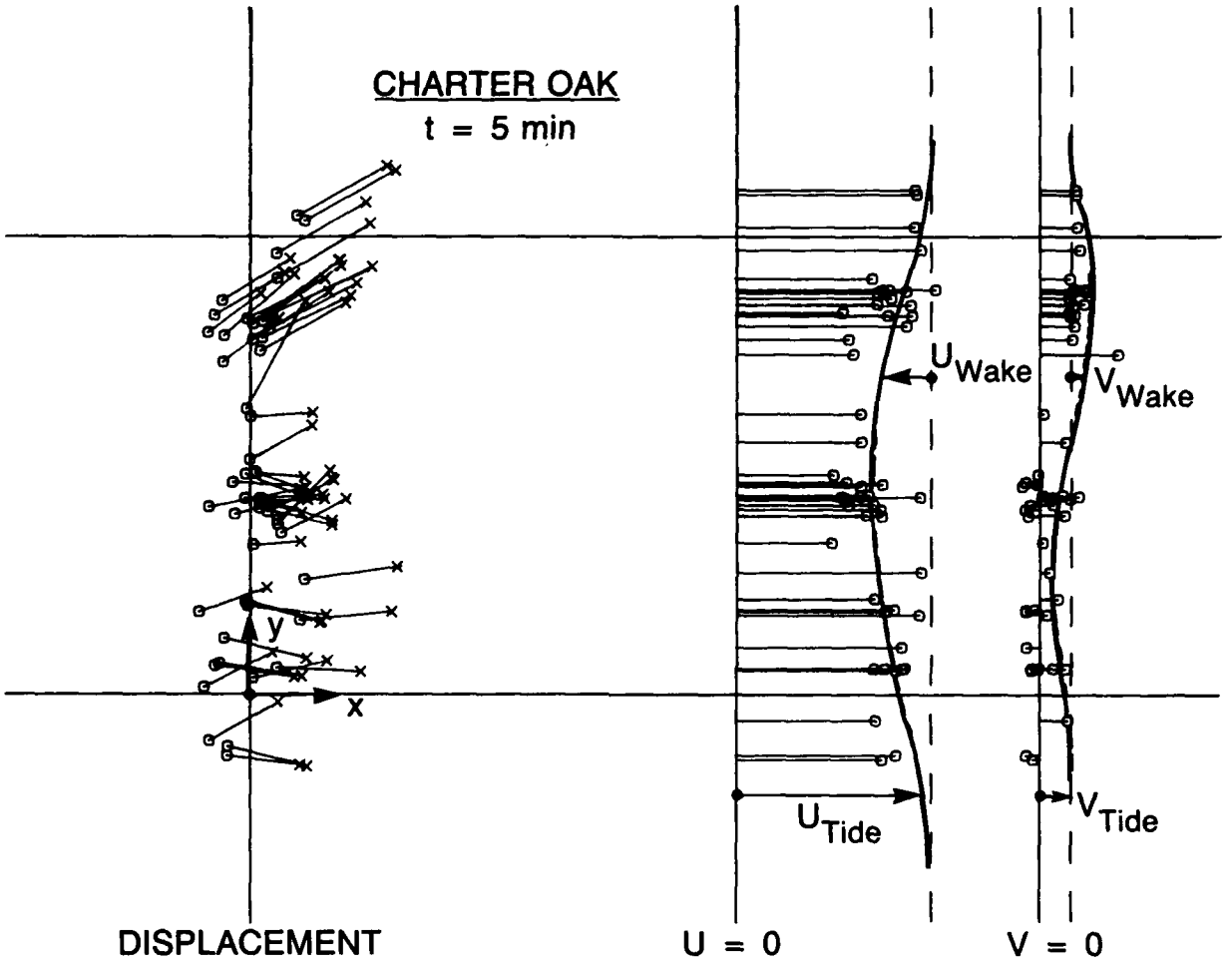

Fig. 3.4 — Marker displacements and velocity components in wake of CHARTER OAK 5 min after ship passage

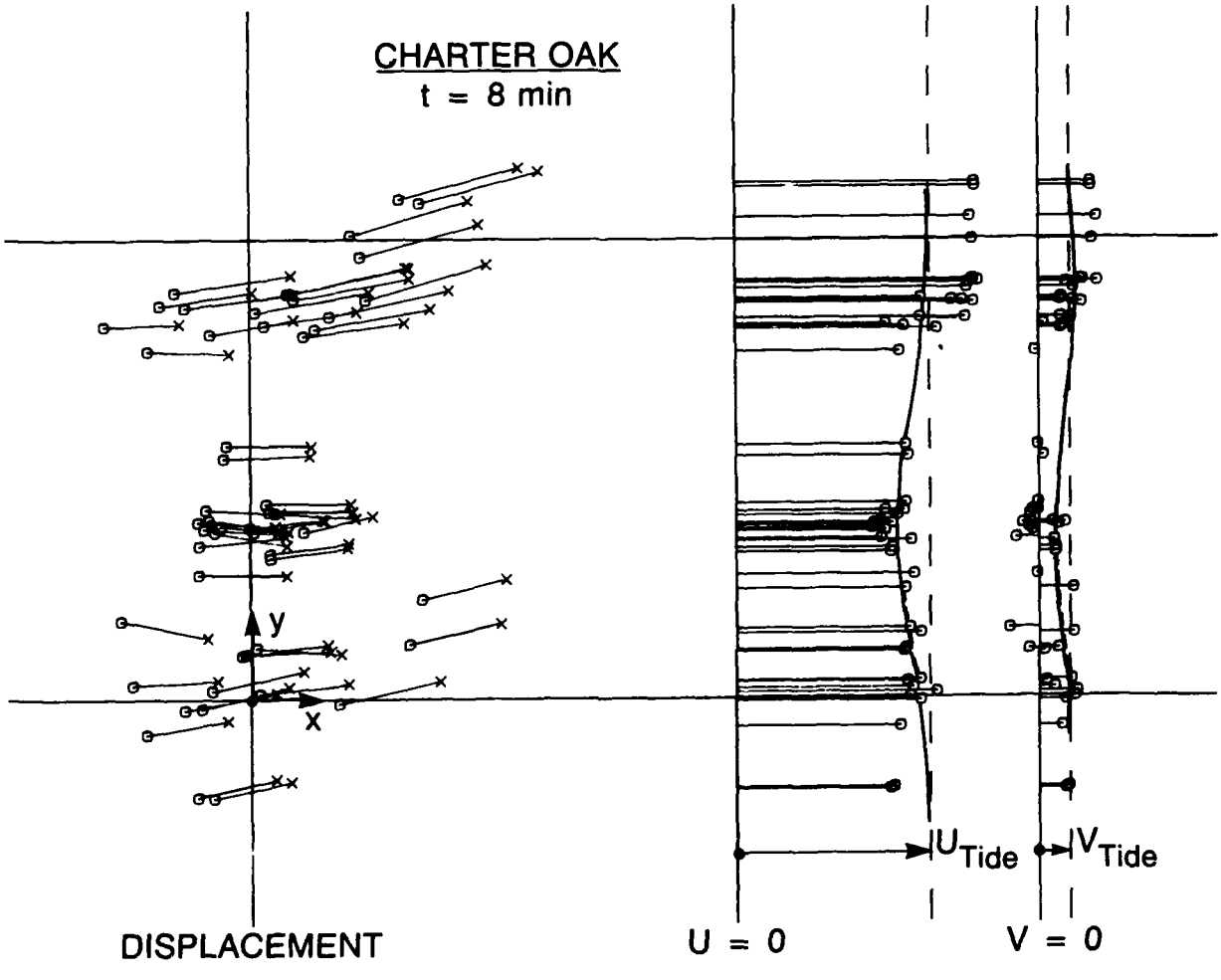

Fig. 3.5 — Marker displacements and velocity components in wake of CHARTER OAK 8 min after ship passage

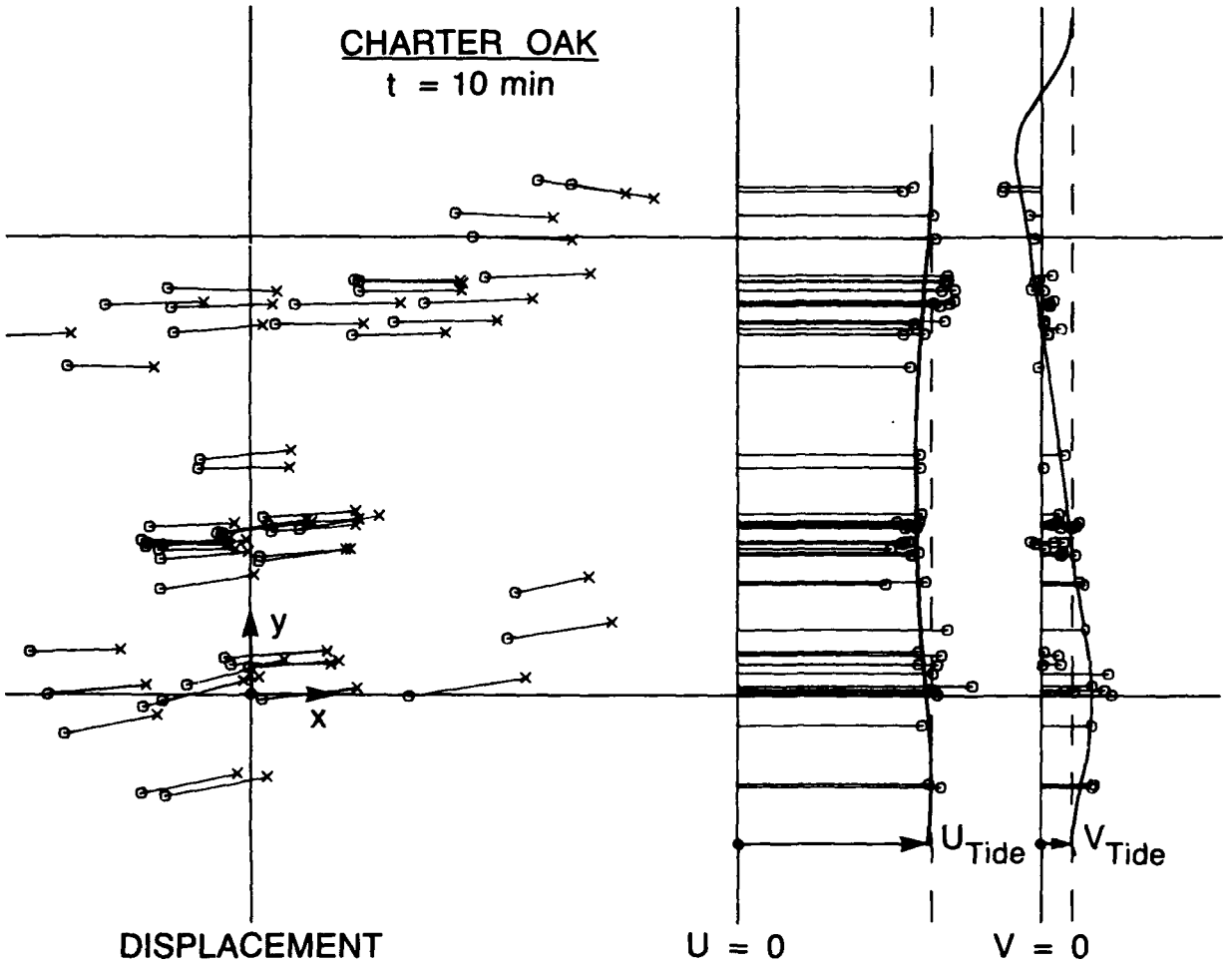

Fig. 3.6 — Marker displacements and velocity components in wake of CHARTER OAK 10 min after ship passage

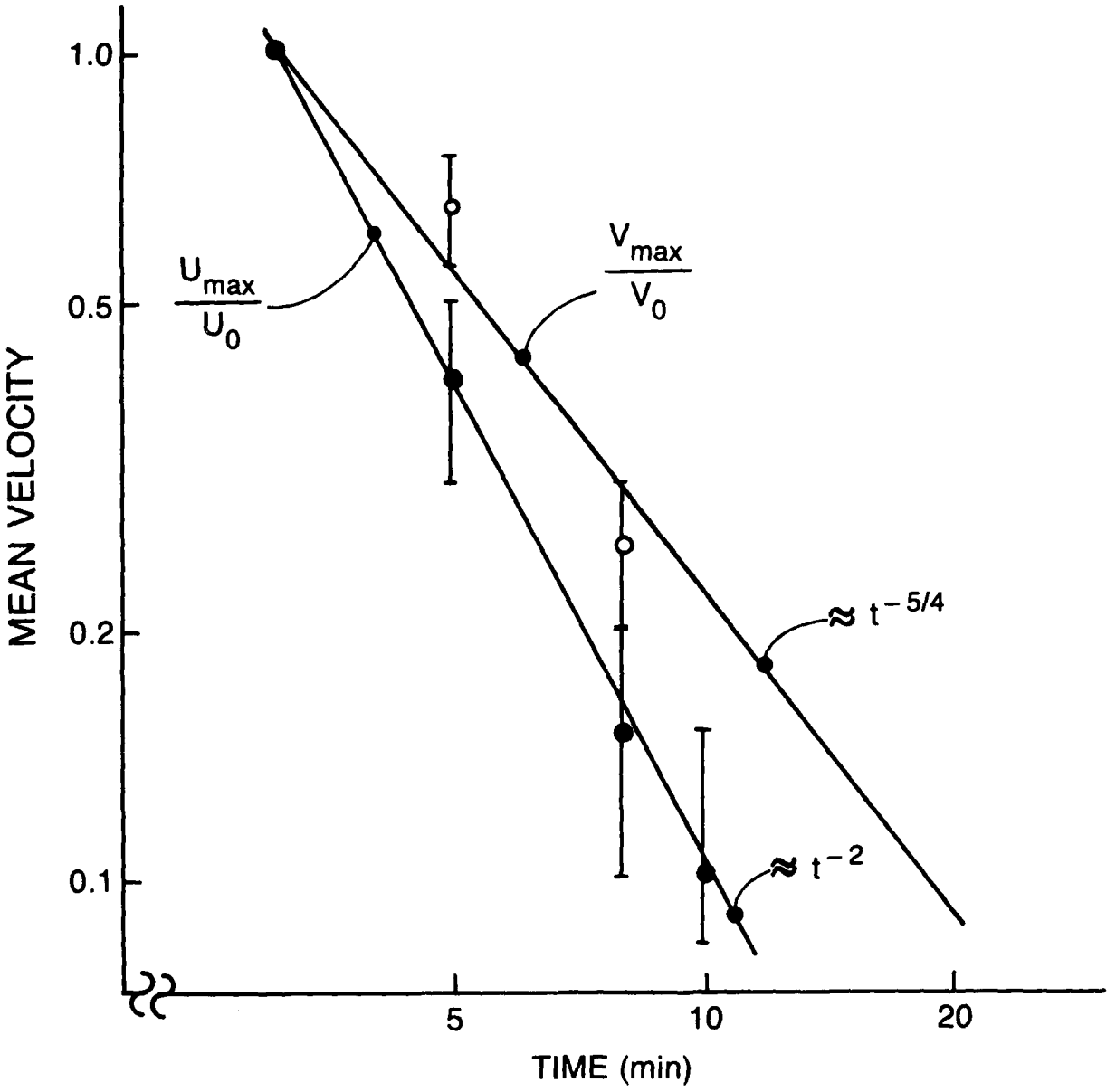

Fig. 3.7 — Decay of maximum axial (U_m) and transverse (V_m) ship wake velocities for the CHARTER OAK

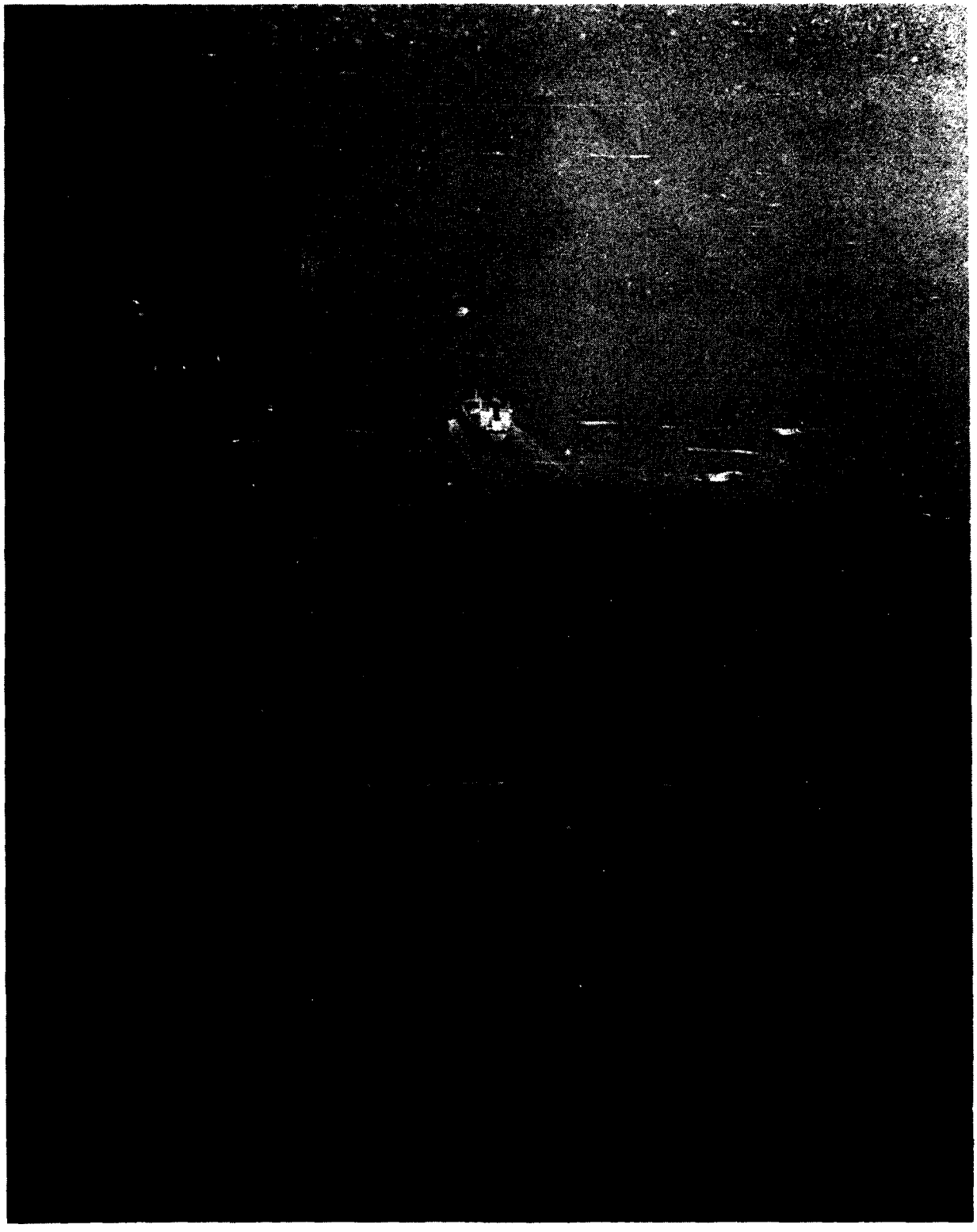

Fig. 3.8a — A sequence of photos showing the evolution of the wake, foam, and edge bands during the surface tension measurements made on the CHARTER OAK wake

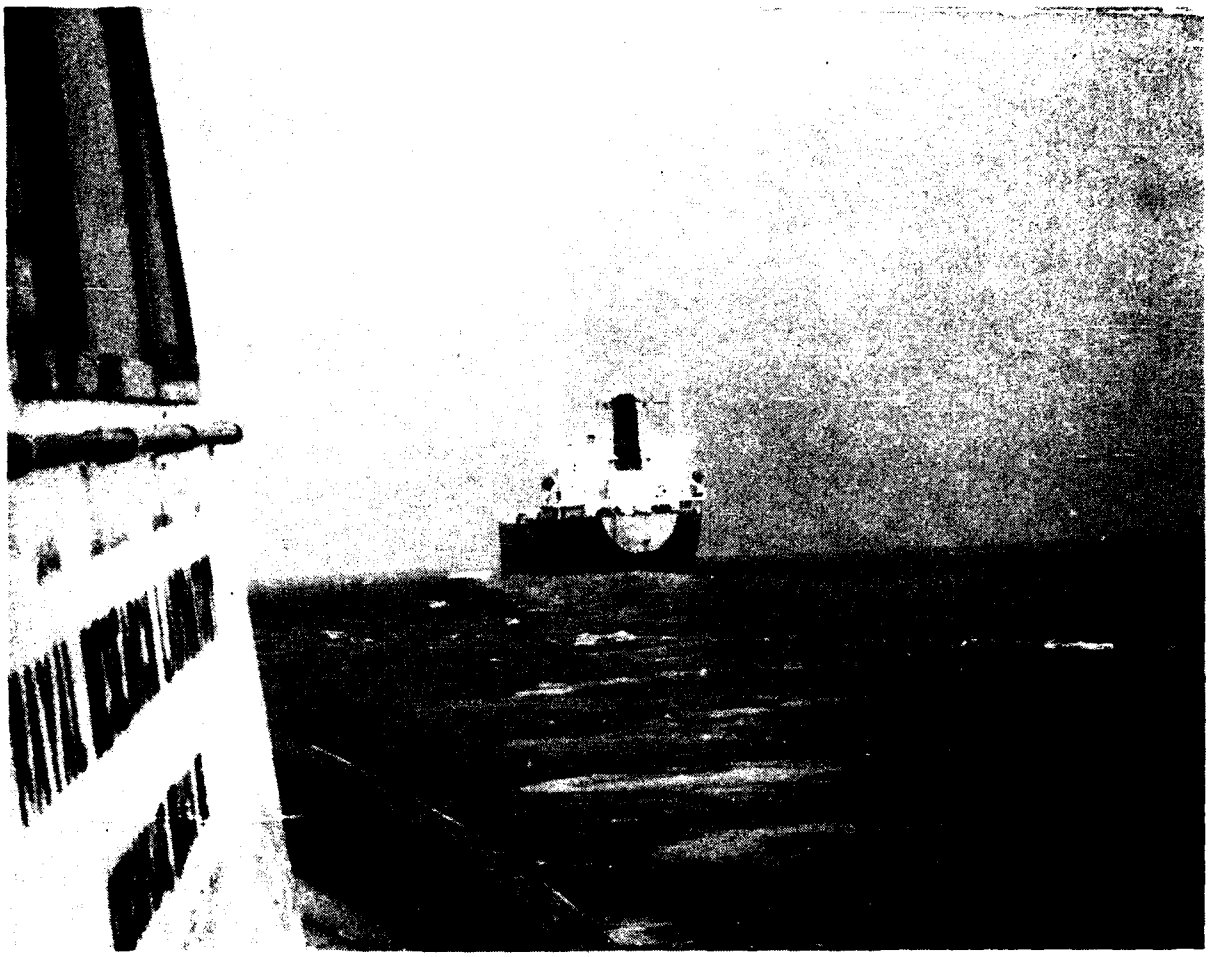

Fig. 3.8b — A sequence of photos showing the evolution of the wake, foam, and edge bands during the surface tension measurements made on the CHARTER OAK wake about 2 min after passage

Fig. 3.8c — A sequence of photos showing the evolution of the wake, foam, and edge bands during the surface tension measurements made on the CHARTER OAK wake nearly 8 min after passage

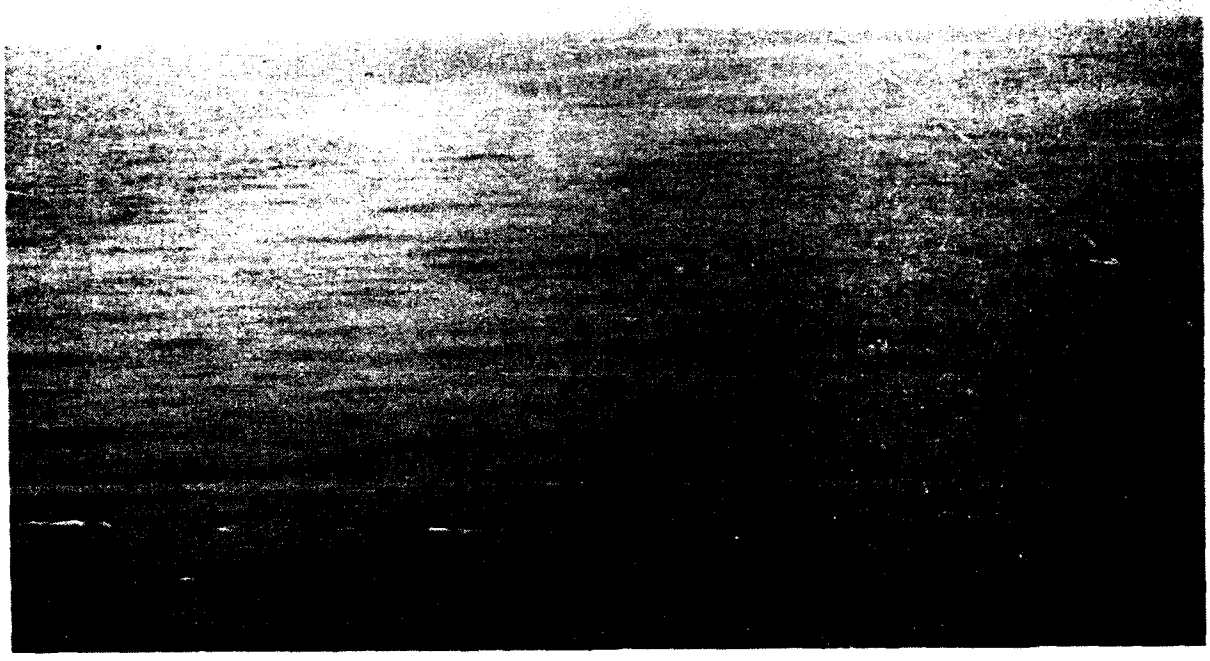

Fig. 3.8d — A sequence of photos showing the evolution of the wake, foam, and edge bands during the surface tension measurements made on the CHARTER OAK wake about 15 min after passage

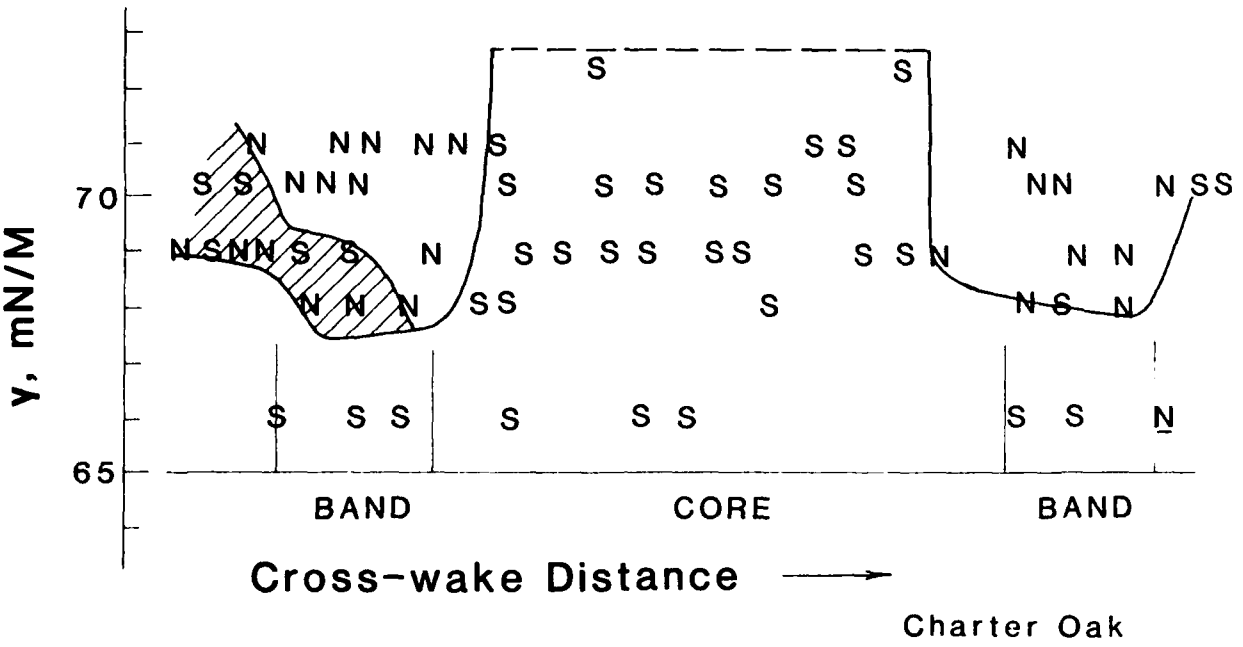

Fig. 3.9 — The spatial variation of surface tension(γ) across the wake of the CHARTER OAK. The curve separating the *N*'s from the *S*'s is the surface tension as a function of cross-wake distance. The shaded region on the left represents observed variability of about 2mN/m in the measurements.

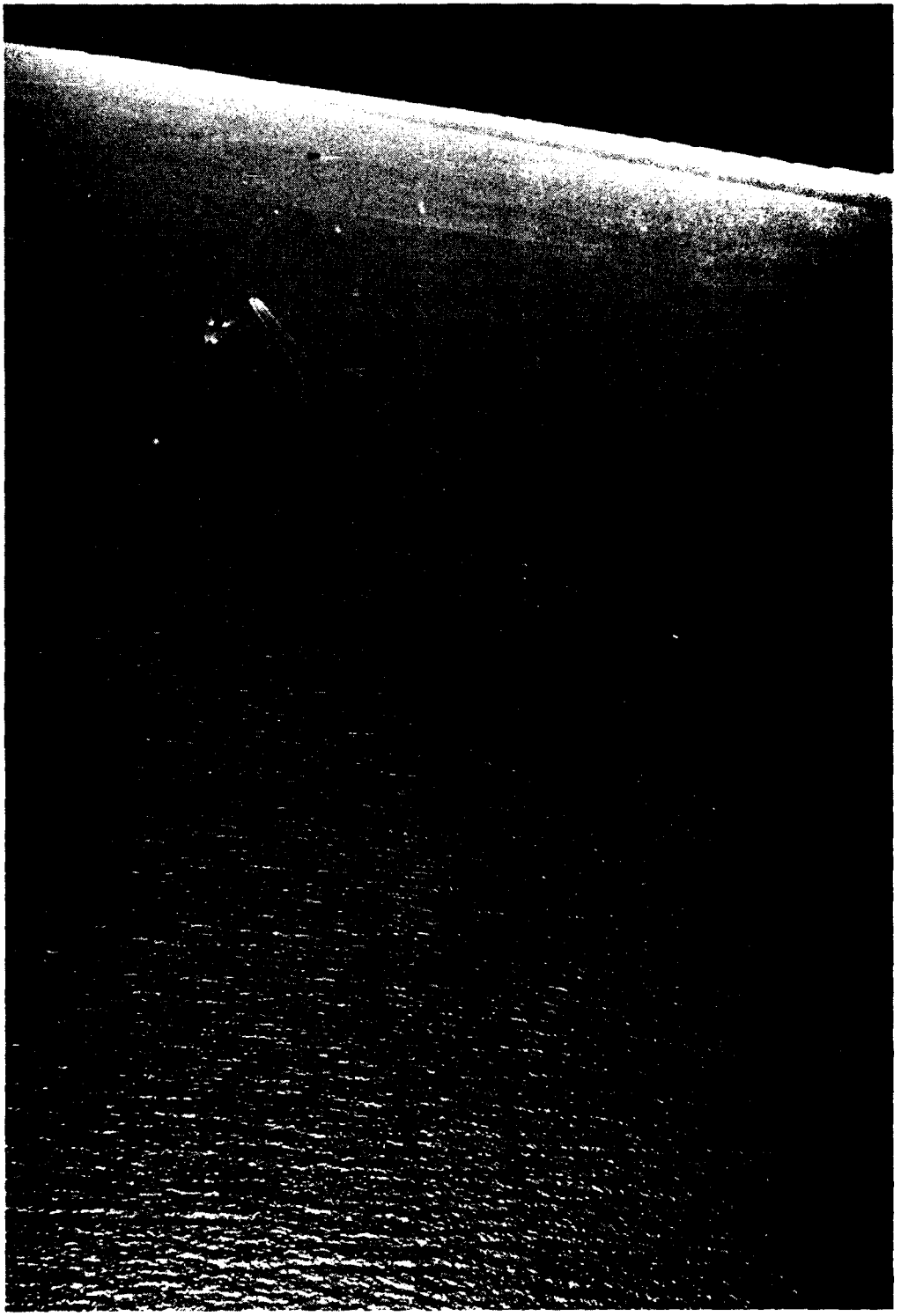

Fig. 3.10 — A slant photo of the LELAND B wake showing the edge bands as the two reflective stripes which merge into the foam bands generated by the bow wave

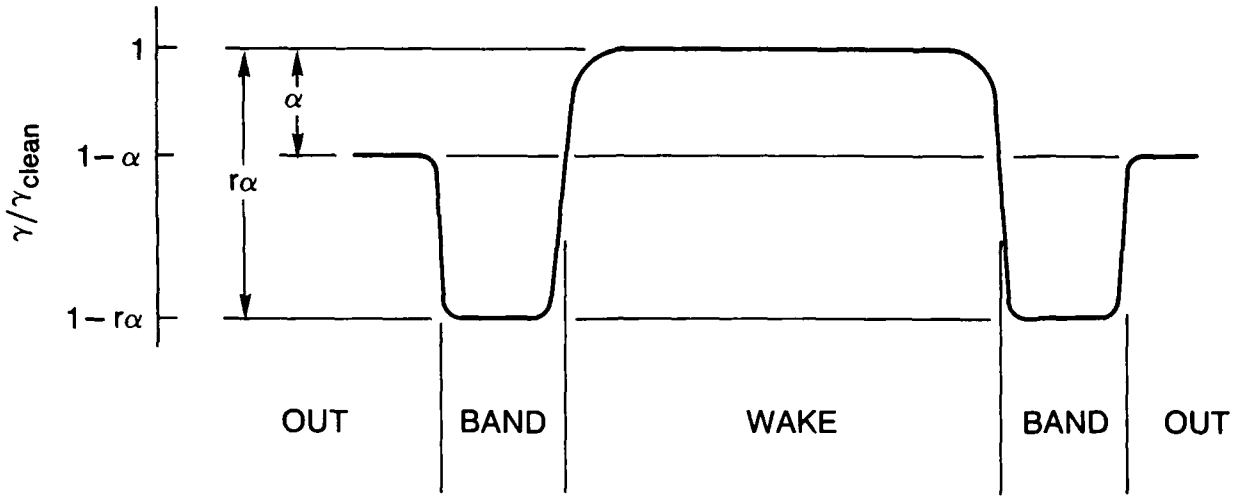

$$\alpha = \frac{\pi_{amb.}}{\gamma_{clean}} = 1 - \frac{\gamma}{\gamma_{clean}}$$

TYPICALLY r = 2

Fig. 3.11 — A proposed parameterized variation of surface tension (γ) across a displacement-hull wake based on our measurements

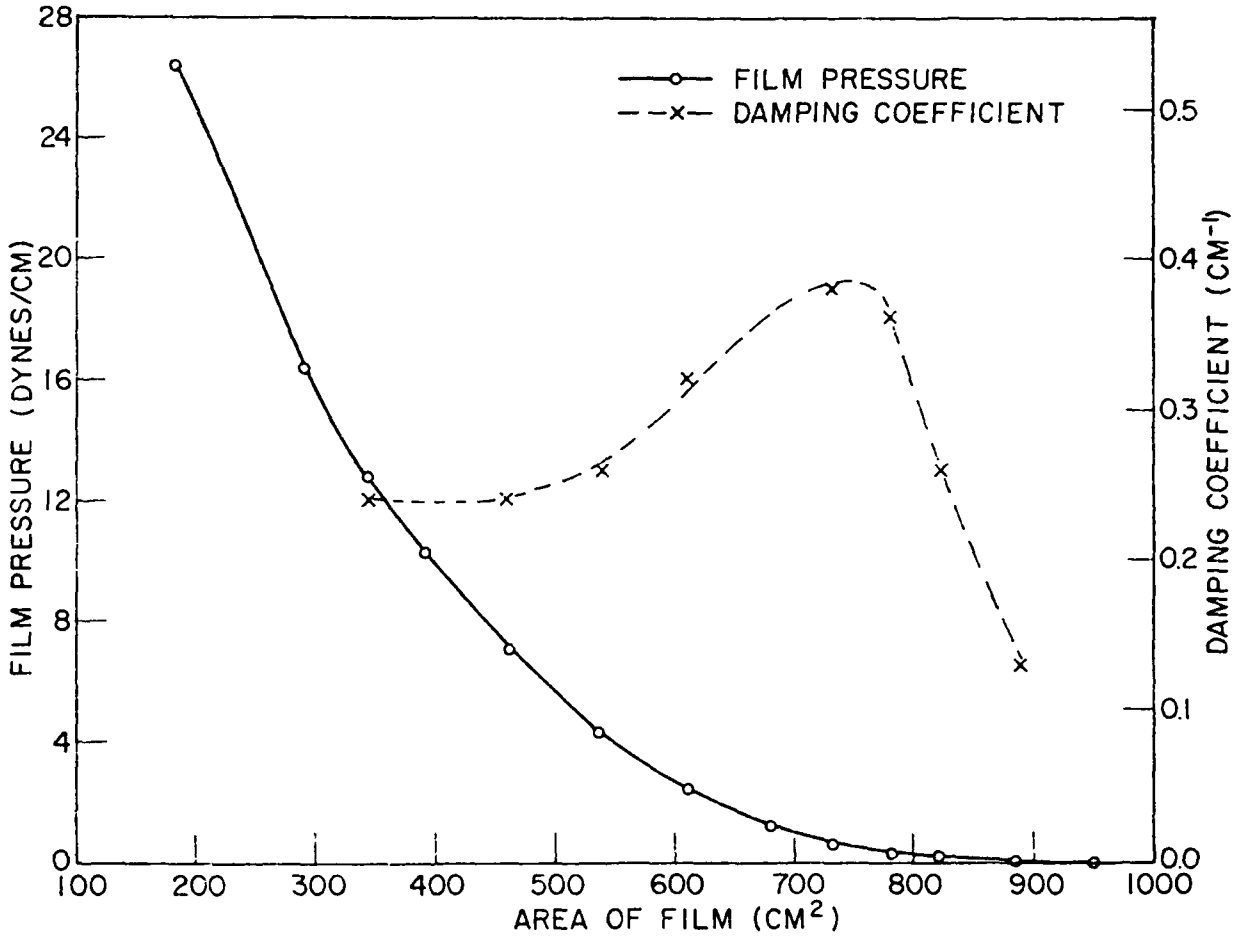

Fig. 3.12 — Film pressure, area-curve for a natural surfactant film from Garrett 1967b. Also shown is the change in damping coefficient for 60 Hz capillary waves as the film area decreases. This capillary wave damping causes compacted films to appear as slicks.

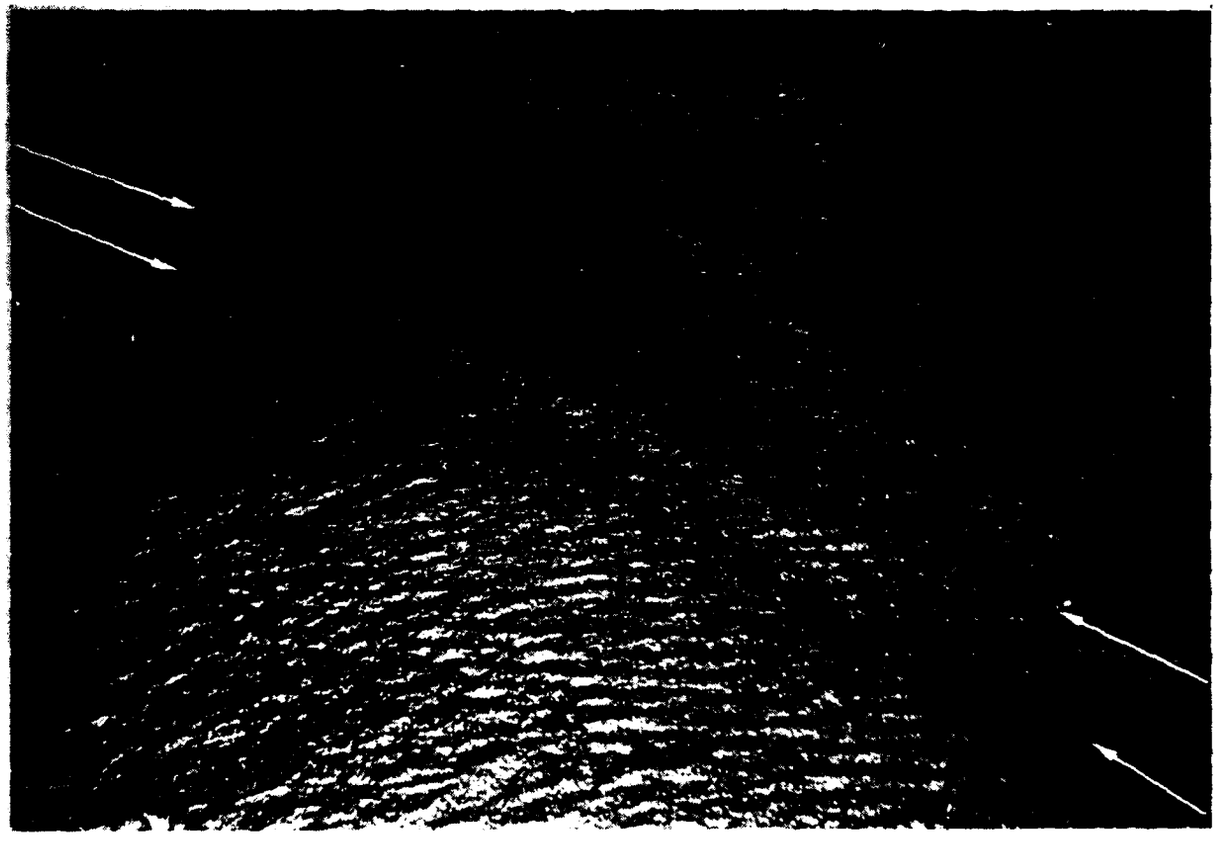

Fig. 3.13 — A partial sun-glint photo of the LELAND B wake. The boat has progressed from right-lower to left-upper. The two edge bands appear as stripes of reduced specular reflection while toward the left edge of the photo bands of residual foam from the wake can be seen in each edge band.

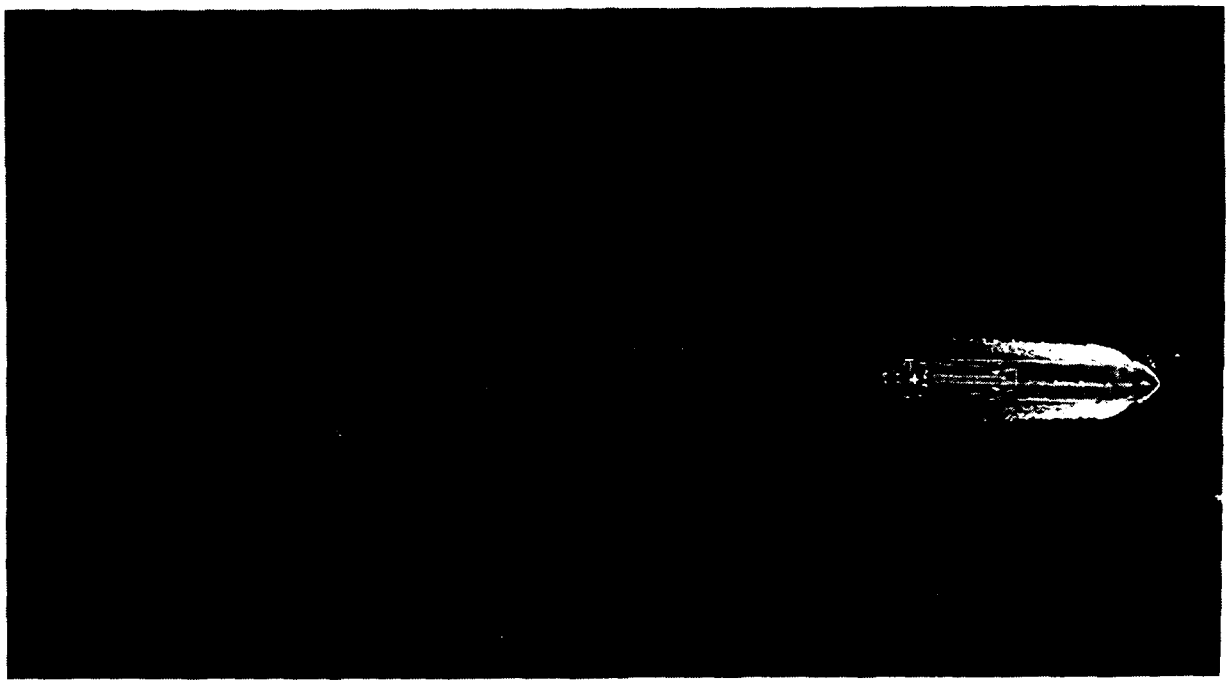

Fig. 3.14 — Survey camera photograph of the visible white water and foam wake of the CHARTER OAK

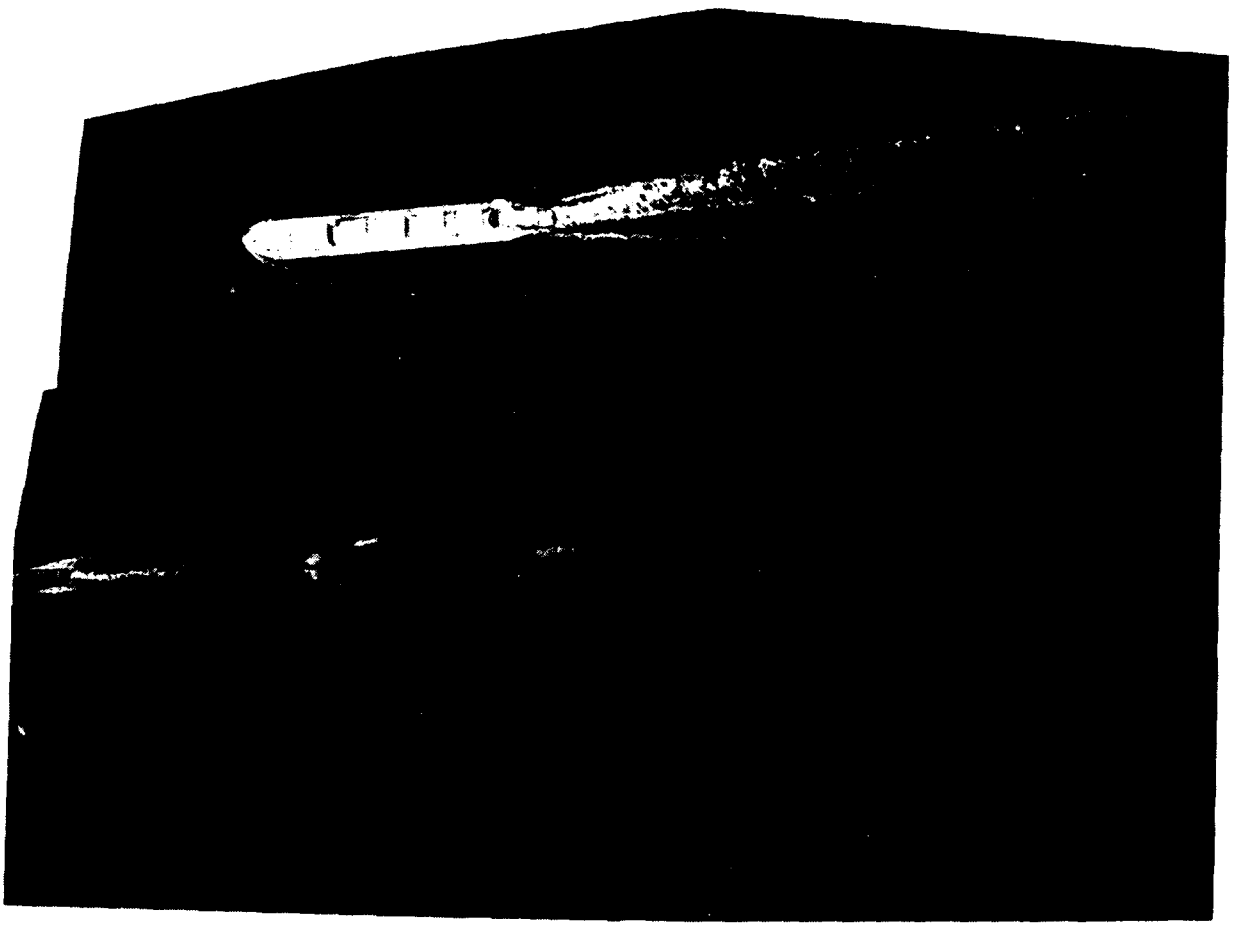

Fig. 3.15 — Comparison of the visible white water and foam wakes of two similar barges with one in tow and with one being pushed. This gives very different propulsion conditions.

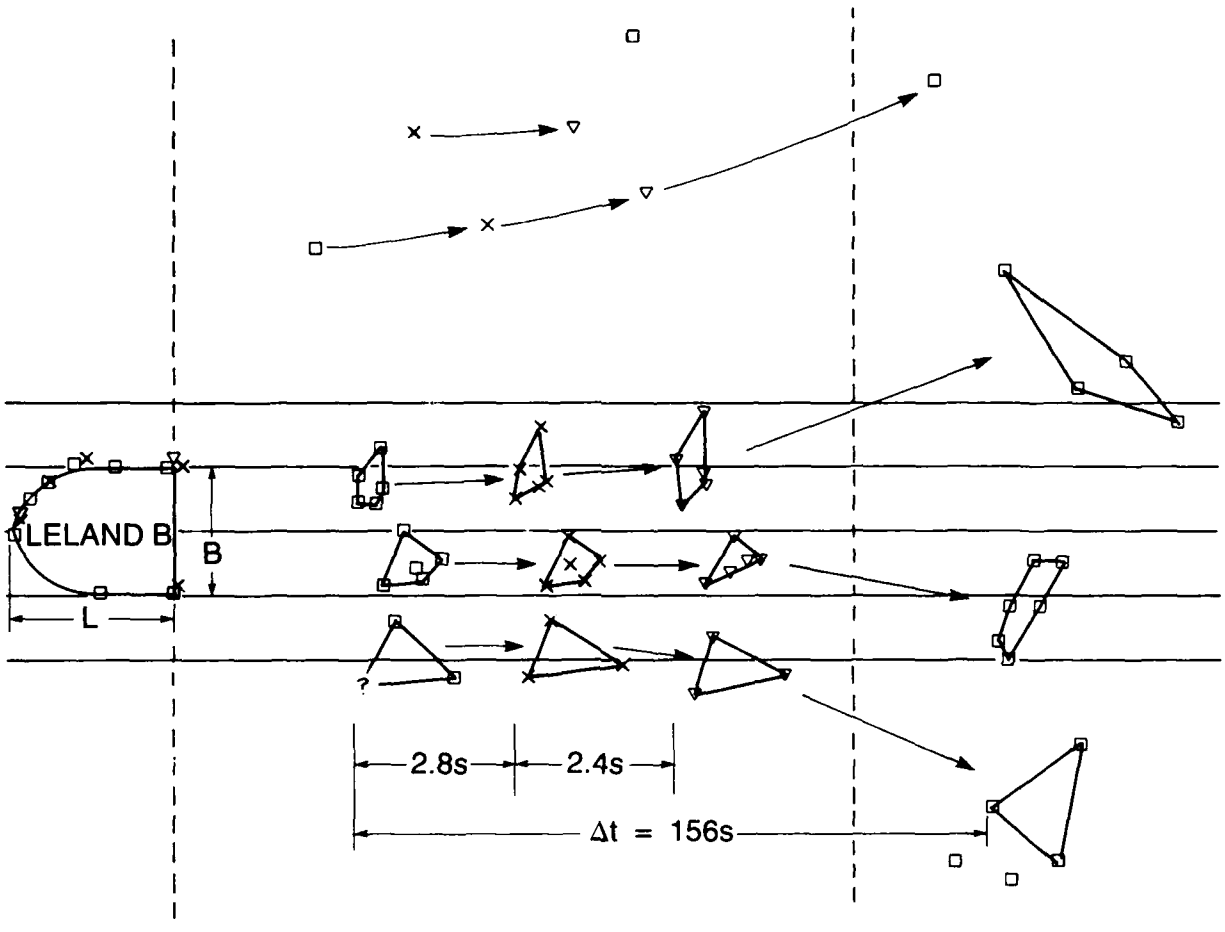

Fig. 3.16 — LELAND B marker locations at four times late showing diffusion but no apparent lateral flows

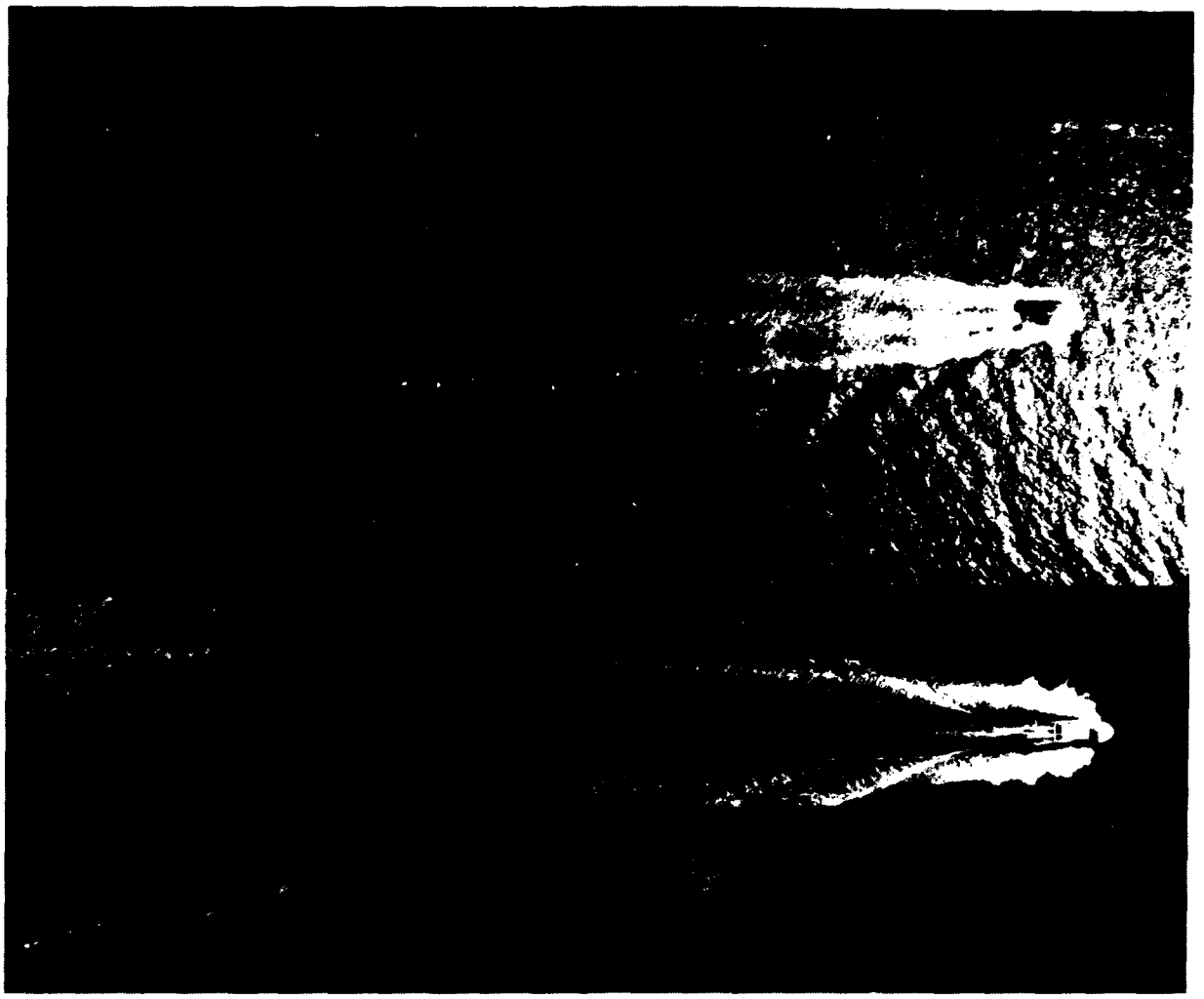

Fig. 3.17 — Small boat photographs of the visible white water and foam wakes of the SHADY LADY (upper), in a planing condition, and the LELAND B (lower), in a displacement hull condition

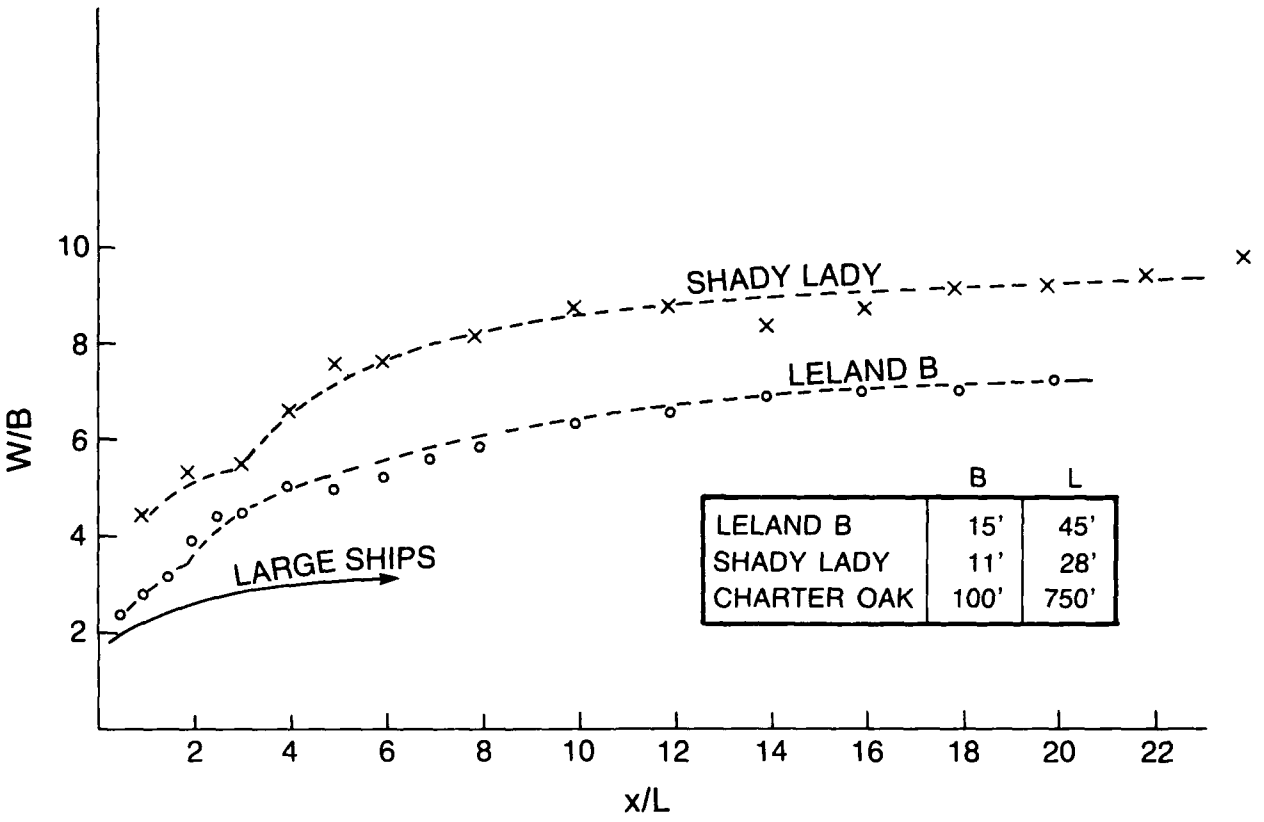

Fig. 3.18 — Visible wake widths W normalized by ship beam, B, and ship length, L

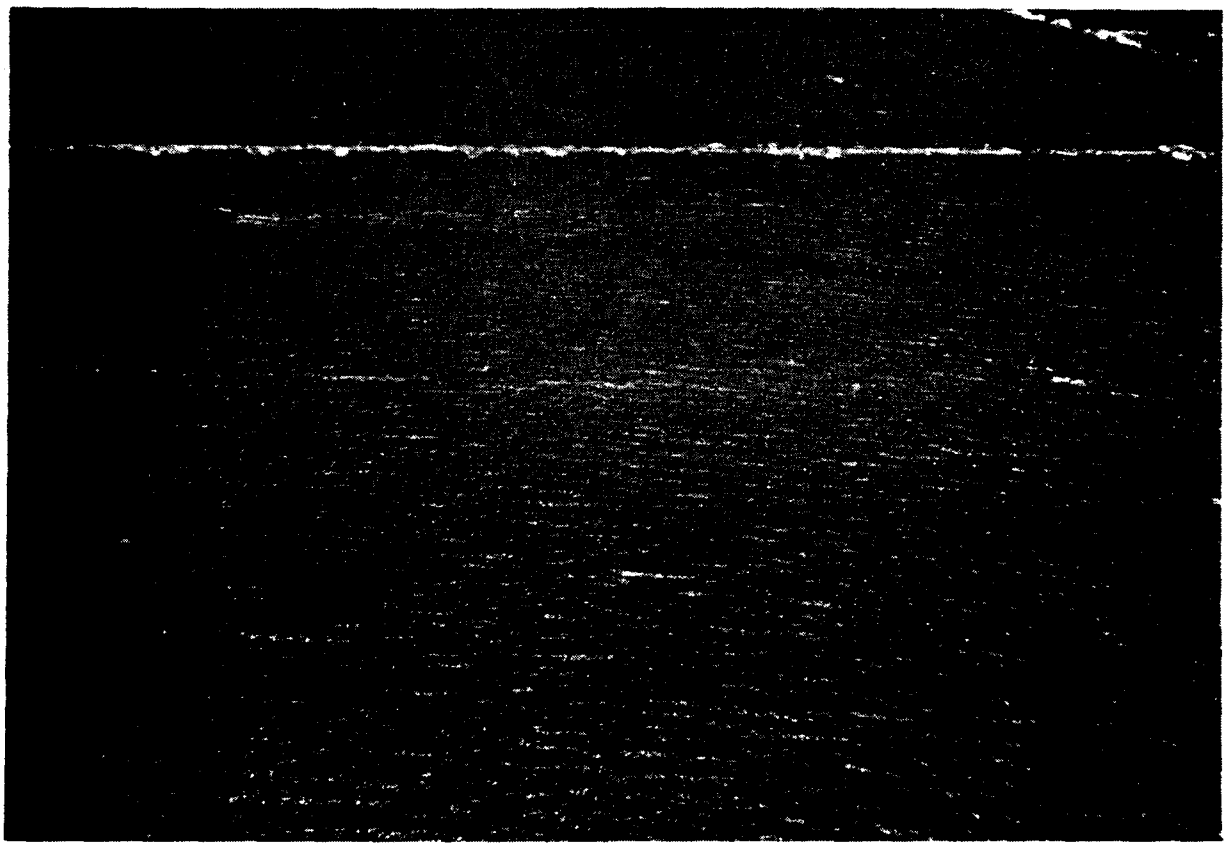

Fig. 3.19 — The LELAND B laying out an artificial slick of oleyl alcohol

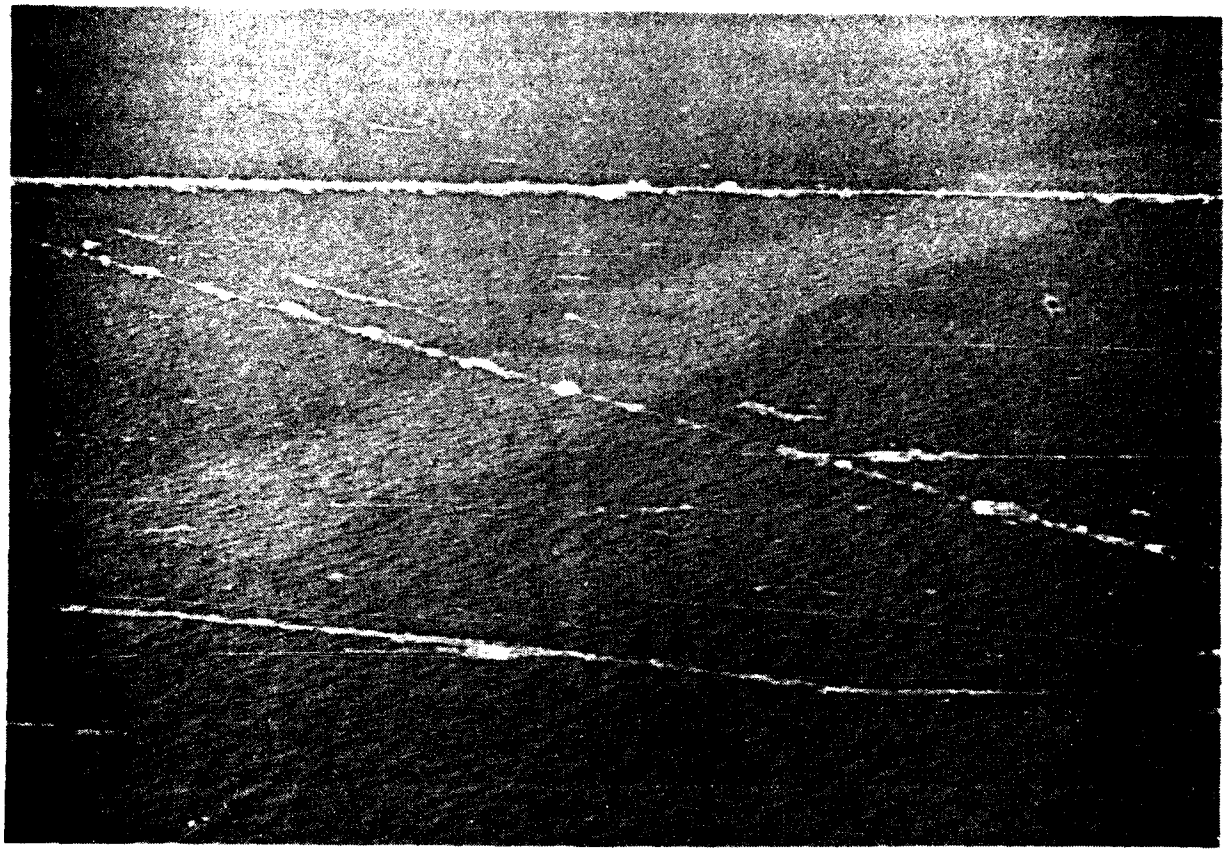

Fig. 3.20 — An artificial slick, 11 min old. The wind speed was 6 to 8 m/s at the time, and the upper-wind side (towards left) is beginning to break up.

(a)

(b)

(c)

Fig. 3.21 — A sequence showing the parting of an artificial slick as a result of the LELAND B being driven through it. After 9 min the cuts are still visible suggesting some secondary flow in the wake may be stressing the surface enough to counteract the natural tendency of the slick material to flow back into the wake region.

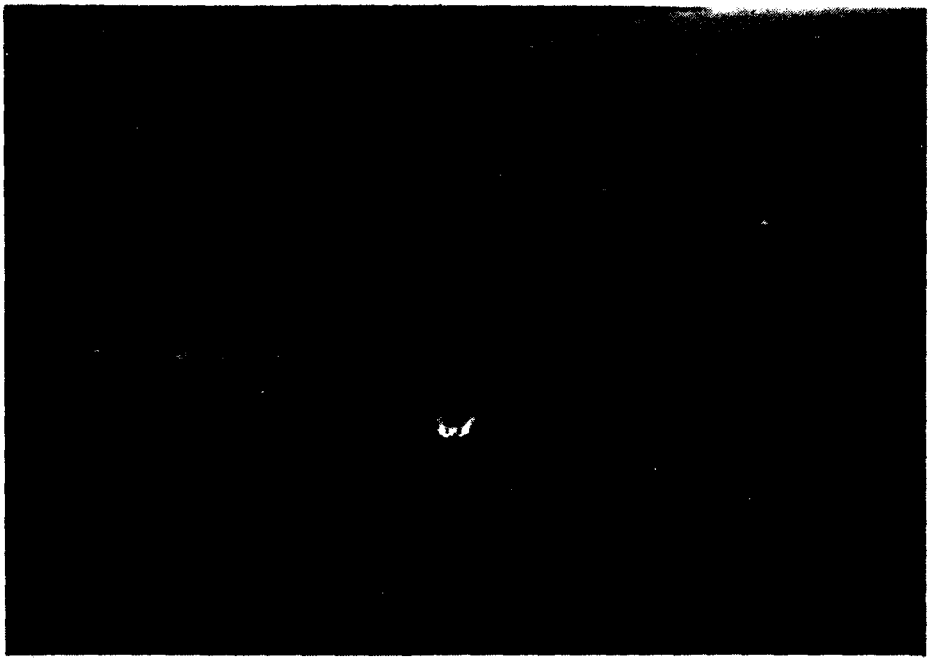

(a)

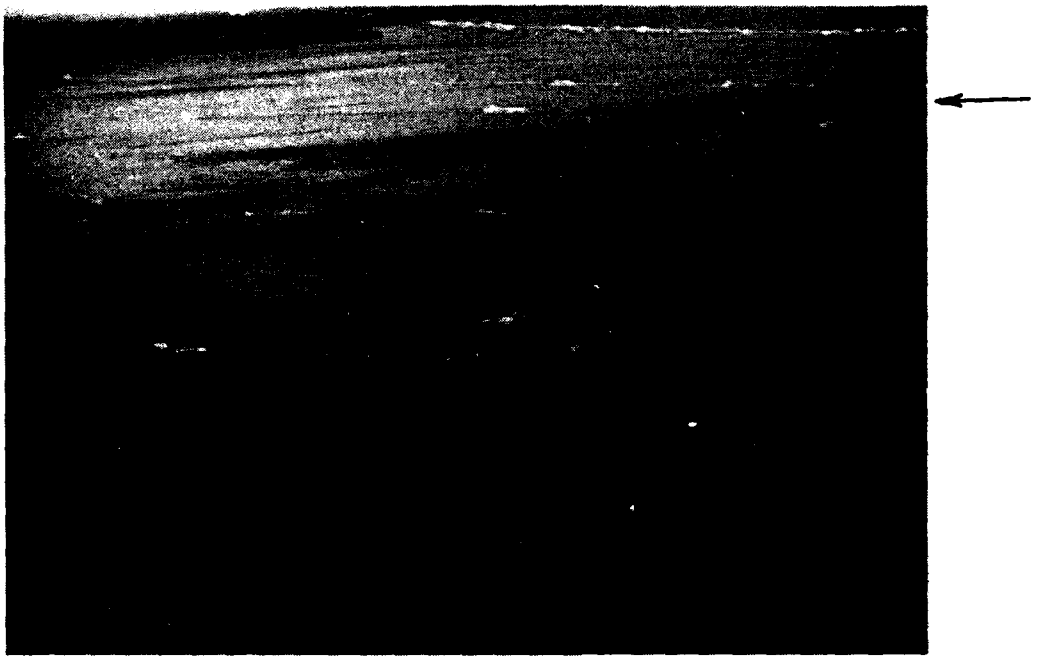

(b)

Fig. 3.22a,b — A sequence of photos showing the LELAND B proceeding through an artificial slick and the wake scars which persist 11 min later

(c)

(d)

Fig. 3.22c,d — A sequence of photos showing the LELAND B proceeding through an artificial slick and the wake scars which persist 11 min later

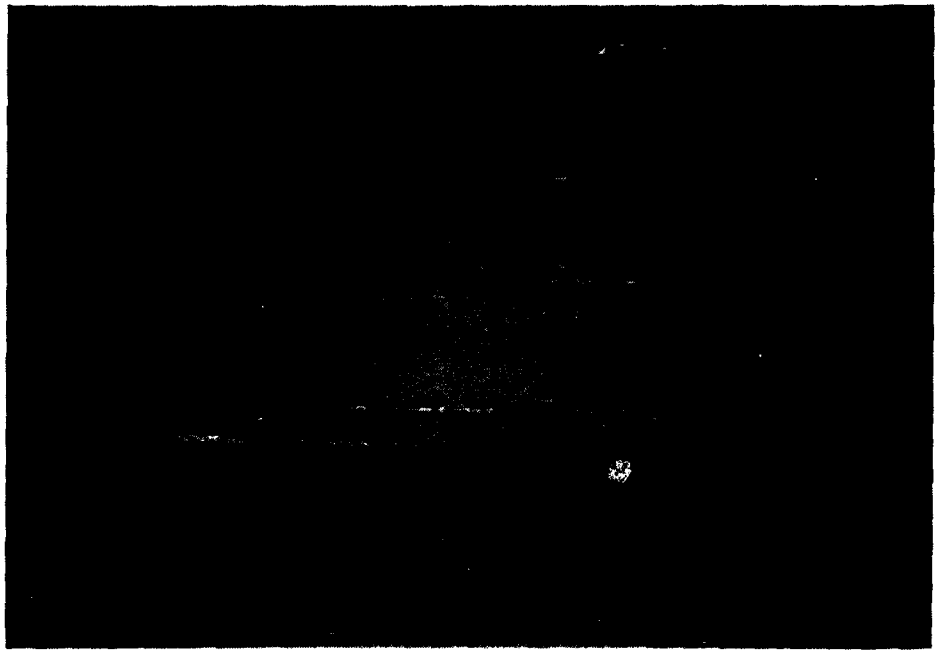

Fig. 3.23 — Residual ship wake scars in an artificial slick

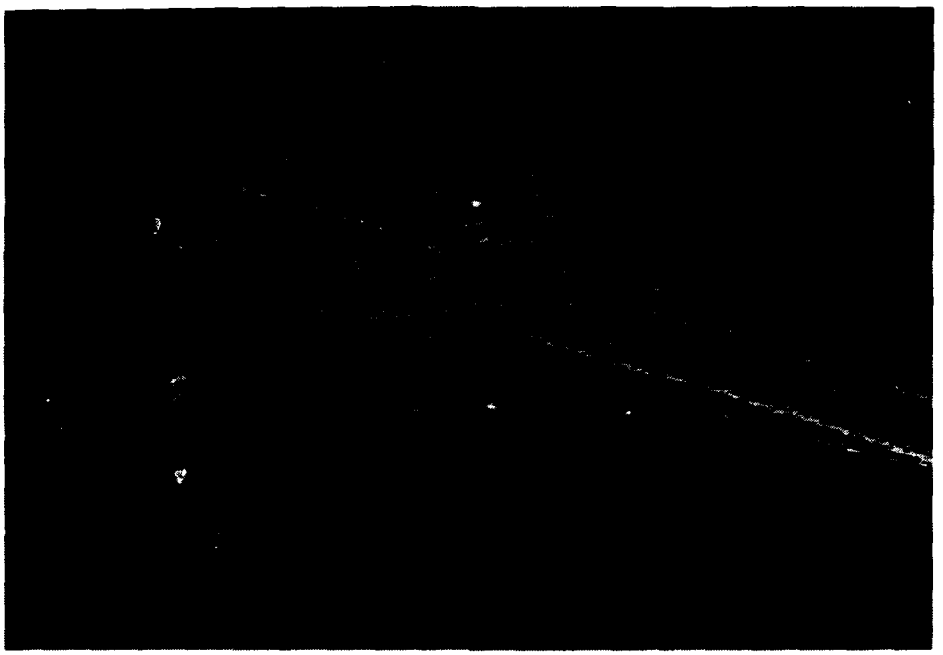

(a)

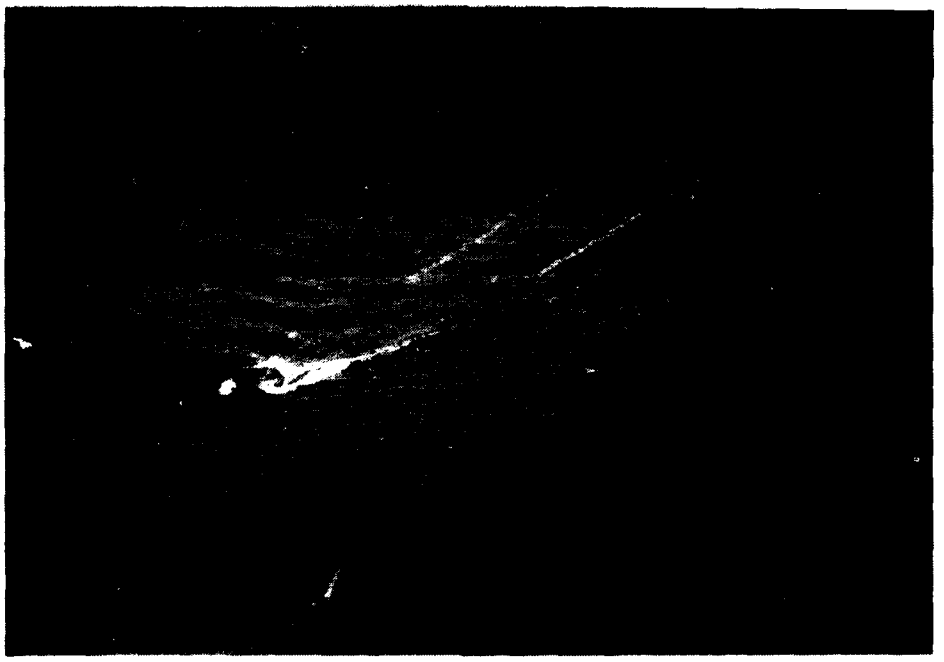

(b)

Fig. 3.24 -- Photos of the wake of the LELAND B just after crossing an artificial slick. Note the suppression of wake foam by the slick.

(a)

(b)

Fig. 3.25a,b — A sequence showing the LELAND B and her wake just as she is crossing an artificial slick

(c)

(d)

Fig. 3.25c,d — The suppression of foam is particularly evident. Notice the unusual wake wave pattern above and to the right (as viewed in the photos) of the wake. It is not clear what mechanism(s) has caused the pattern.

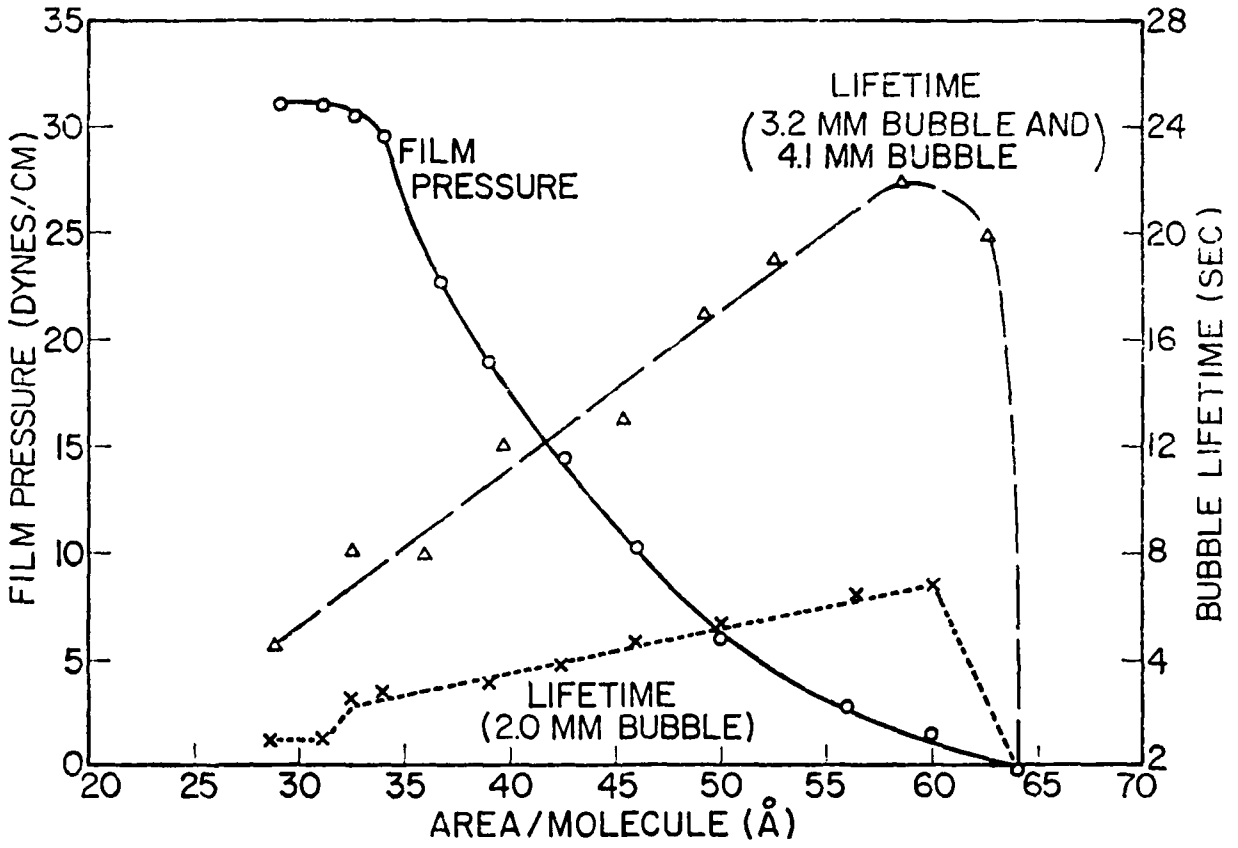

Fig. 3.26 — Bubble lifetime and a pressure, area curve for oleic acid (Garrett, 1967c). Bubbles were generated below the water surface containing the oleic acid film and their residence times (lifetimes) on the surface measured. As the film becomes compacted, the bubble lifetimes decrease significantly. This may explain the foam suppression observed with the artificial slicks.